https://doi.org/10.5194/acp-2021-73
Preprint. Discussion started: 3 March 2021

Atmospheric Chemistry and Physics Discussions

Observation and modeling of a historic African dust intrusion into the Caribbean Basin and the southern U.S. in June 2020

Hongbin Yu[1], Qian Tan[2,3], Lillian Zhou[1], Yaping Zhou[1,4], Huisheng Bian[1,4], Mian Chin[1], Claire L. Ryder[5], Robert C. Levy[1], Yaswant Pradhan[6], Yingxi Shi[1,4], Qianqian Song[4,7], Zhibo Zhang[4,7], Peter R. Colarco[1], Dongchul Kim[1,8], Lorraine A. Remer[4], Tianle Yuan[1,4], Olga Mayol-Bracero[9], Brent N. Holben[1]

[1]Earth Sciences Division, NASA Goddard Space Flight Center, Greenbelt, MD, USA
[2]Bay Area Environment Research Institute, Petaluma, CA, USA
[3]Earth Science Division, NASA Ames Research Center, Moffett Field, CA, USA
[4]JCET, University of Maryland at Baltimore County, Baltimore, MD, USA
[5]Department of Meteorology, University of Reading, Reading, RG6 6BB, UK
[6]Met Office, Exeter, EX1 3PB, UK
[7]Physics Department, University of Maryland at Baltimore County, Baltimore, MD, USA
[8]GESTAR, Universities Space Research Association, Columbia, MD, USA
[9]University of Puerto Rico, Puerto Rico, USA

Correspondence to: Hongbin Yu (Hongbin.Yu@nasa.gov)

Abstract. This study characterizes a massive African dust intrusion into the Caribbean Basin and southern U.S. in June 2020, which is nicknamed the "Godzilla" dust plume, using a comprehensive set of satellite and ground-based observations (including MODIS, CALIOP, SEVIRI, AERONET, and EPA Air Quality network) and the NASA GEOS global aerosol transport model. The MODIS data record registered this massive dust intrusion event as the most intense episode over the past two decades. During this event, the aerosol optical depth observed by AERONET and MODIS peaked at 3.5 off the coast of West Africa and 1.8 in the Caribbean Basin. CALIOP observations show that the top of dust plume reached altitudes of 6-8 km in West Africa and descended to about 4 km altitude over the Caribbean Basin and 2 km over the U.S. Gulf coast. The dust plume degraded the air quality in Puerto Rico to the hazardous level, with maximum daily PM_{10} concentration of 453 μg m^{-3} recorded on June 23. The dust intrusion into the U.S. raised the $PM_{2.5}$ concentration on June 27 to a level exceeding the EPA air quality standard in about 40% of the stations in the southern U.S. Satellite observations reveal that dust emissions from convection-generated haboobs and other sources in West Africa were large albeit not extreme on a daily basis. However, the anomalous strength and northern shift of the North Atlantic Subtropical High (NASH) together with the Azores low formed a closed circulation pattern that allowed for accumulation of the dust near the African coast for about four days. When the NASH was weakened and wandered back to south, the dust outflow region was dominated by a strong African Easterly Jet that rapidly transported the accumulated dust from the coastal region toward the Caribbean Basin, resulting in the record-breaking African dust intrusion. In comparison to satellite observations, the GEOS model well reproduced the MODIS observed tracks of the

https://doi.org/10.5194/acp-2021-73
Preprint. Discussion started: 3 March 2021


Atmospheric Chemistry and Physics Discussions

meandering dust plume as it was carried by the wind systems. However, the model substantially underestimated dust emissions from haboobs and did not lift up enough dust to the middle troposphere for ensuing long-range transport. Consequently, the model largely missed the satellite-observed elevated dust plume along the cross-ocean track and underestimated the dust intrusion into the Caribbean Basin by a factor of more than 4. Modeling improvements need to focus on developing more realistic representations of moist convection, haboobs, and the vertical transport of dust.

1 Introduction

Trans-Atlantic transport of African dust to the Caribbean Basin and the Americas is a year-round phenomenon *[Yu et al., 2013; Prospero et al., 2014]* that imposes far-reaching impacts on air quality and human health, the radiation budget, clouds and weather systems, soil development, snow melting, and terrestrial and aquatic ecosystems (Swap et al., 1992; Prospero, 1999; DeMott et al., 2003; Miller et al., 2004; Okin et al., 2004; Jickells, et al., 2005; Chin et al., 2007; Muhs et al., 2007; Evan et al., 2011; Yu et al., 2015b; Yuan et al., 2016; Song et al., 2018; Tao et al., 2018). On average, it has been estimated that about 180 million tons of dust from North Africa are carried by the trade winds each year to sweep across the tropical North Atlantic Ocean. This dust lands in different parts of the Americas and the Caribbean Basin (Yu et al., 2015a), which is modulated by the seasonal migration of the intertropical convergence zone (ITCZ).

Dust uplift during the Saharan summertime dust season is primarily driven by two mechanisms: Low Level Jets (LLJs) and haboobs (Marsham and Ryder, 2021). LLJs occur when nocturnal jets are mixed down towards the surface as the daytime boundary layer develops with surface heating. Haboobs occur due to cold-pool outflows in the form of density currents from convective systems, with high wind speeds and dust uplift. These high-wind events play important role in dust lifting and make the largest contribution to interannual variability of dust generation (Cowie et al., 2015). Marsham et al. (2013) found that haboobs accounted for as much as 50% of Saharan summertime dust uplift. Convective mixing resulting from intense solar heating gradually mixes dust vertically as the convective boundary layer grows, eventually mixing it throughout the entire Saharan boundary layer up to 6-8 km (e.g., Engelstaedter et al., 2015; Ryder et al. 2015). Easterly mid-level winds then advect the dust westwards over the Atlantic Ocean, where it overrides the marine boundary layer becoming the elevated Saharan Air Layer (SAL) (e.g., Karyampudi 1999; Carlson and Prospero 1972).

It is worth noting that these dust events are episodic in nature and vary substantially in intensity from event to event. Because of the high intensity and broad reach of extreme dust events, they can impose enormous albeit intermittent impacts on the environment on a large spatial scale. Often a few extreme dust events could make disproportionally large contributions to the annual dust budget. It is thus important to characterize such extraordinary events with comprehensive observations and understand their underlying processes. It is also critical to assess to what extent global aerosol models can capture such extreme intercontinental transport events.

In late June 2020, a gigantic dust plume was observed to intrude into the Caribbean Basin and the southern U.S. **Figure 1** shows a snapshot panorama of dust plumes observed at 14:47:32 GMT on June 23, 2020, taken by the Earth Polychromatic Imaging Camera (EPIC) onboard the Deep Space Climate Observatory (DSCOVR) at the first Lagrange point (L1) between

https://doi.org/10.5194/acp-2021-73
Preprint. Discussion started: 3 March 2021


Atmospheric Chemistry and Physics Discussions

Earth and the sun (about one and a half million miles above the Earth's surface) (Marshak et al., 2018). Featured in the image is a dense dust plume over the Caribbean Basin followed by another just off the African coast in the eastern North Atlantic Ocean. These two dust plumes are about 5000 km apart but appears to be comparable in the intensity. The dust over the Caribbean Basin during this period has attracted considerable interests from scientific community and media because of its huge extent and massive amount, so-called the "Godzilla" dust plume (https://phys.org/news/2020-06-sahara-blankets-caribbean-air-quality.html), and "a dust plume to remember" (https://earthobservatory.nasa.gov/images/146913/a-dust-plume-to-remember) for its extraordinary characteristics. Francis et al. (2020) examined the atmospheric circulation characteristics that drove the formation and transport of this dust storm. In this study, we will use a variety of remote sensing and in situ observations and simulations with the NASA Goddard Earth Observing System (GEOS) model to characterize the gigantic dust plume and assess its impact on the air quality in the southern U.S. Specifically, we will: (1) characterize the evolution of the three-dimensional structure of the dust plumes along their cross-ocean transit , (2) place the intensity of the "Godzilla dust plume" in a context of the last two decades, (3) understand major synoptic processes that resulted in the gigantic dust intrusion into the Caribbean Basin, (4) assess its impact on particulate matter (PM) air quality in the southern U.S., and (5) evaluate the Goddard Earth Observing System (GEOS) model simulation of the dust event with the observations.

The rest of the paper is organized as follows. Section 2 describes the data and model we use to characterize the dust event, including aerosol retrievals from the Moderate Resolution Imaging Spectroradiometer (MODIS), aerosol vertical profiles from the Cloud-Aerosol Lidar with orthogonal Polarization (CALIOP), surface $PM_{2.5}$ (PM with aerodynamic diameter less than 2.5 μm) concentration from the U.S. Environmental Protection Agency (EPA) air quality network, dust and deep clouds from the Spinning Enhanced Visible and InfraRed Imager (SEVIRI), and aerosol simulations with the model. Section 3 presents major results of the data analysis and addresses several important questions, including: (a) how did the three-dimensional structure of the dust plumes evolved during the trans-Atlantic journey? (b) is this episode a historic event over the past two decades? (c) what are major meteorological factors responsible for the huge dust intrusion? (d) what is the adverse impact of the dust event on the $PM_{2.5}$ air quality in the southern U.S.? and (e) to what extent does the GEOS model capture the observed characteristics and quantities of the dust plume? Major conclusions are summarized in section 4.

2 Description of data and model

2.1 MODIS aerosol optical depth

The MODIS instruments onboard both the NASA Terra (morning) and Aqua (afternoon) satellites, acquire near global, daily observations of aerosols with a wide swath of ~2330 km. Because of its wide spectral range and the simplicity of the dark ocean surface, MODIS dark-target (DT) algorithm (Remer et al., 2005, 2020; Levy et al., 2013) has the capability of retrieving AOD with a relatively high accuracy, as well as information on particle size (in the form of Angstrom exponent, effective radius or fine-mode fraction - FMF). The FMF measures the contribution of fine-mode particles to total AOD at 0.55 μm (Remer et al., 2005). In the operational DT aerosol retrieval dust is assumed to be spherical, which introduces errors in the

https://doi.org/10.5194/acp-2021-73
Preprint. Discussion started: 3 March 2021


Atmospheric Chemistry and Physics Discussions

aerosol retrievals downwind of the dust source regions. Most recently, an enhanced DT retrieval algorithm has been developed to improve dust retrievals by accounting for non-sphericity of dust particles (Zhou et al., 2020a). It has been shown that this enhanced dust retrieval algorithm significantly improves the retrievals of AOD and FMF over ocean (Zhou et al., 2020b). For this study exclusively, the enhanced DT algorithm has been applied to the identified dust scenes over ocean from June 10-30, 2020. Although the DT algorithm is also applied to retrieval AOD over vegetated lands, it does not retrieve aerosol over deserts because of interference of strong surface signal. The Deep Blue (DB) algorithm was initially developed to retrieve AOD and other aerosol properties over bright surfaces and then extended to vegetated lands and oceans *(Hsu et al., 2013)*, which complements the DT retrievals. The DT and DB products have been combined, on the basis of their performance in reproducing the Aerosol Robotic Network (AERONET) observations, to characterize the global aerosol system (Levy et al., 2013). For this study, we aggregate the enhanced DT over-ocean retrievals into 1°x1° grids. Over land, we use MODIS Collection 6.1 daily data. We also combine MODIS AOD at 550 nm from Terra and Aqua to acquire a better spatial coverage of daily aerosol distribution than each satellite alone. When both Terra and Aqua have AOD retrievals, they are averaged. In this study, we will use the AERONET data to validate MODIS AOD retrieval for this intense dust event. The AERONET is a ground-based network with equipped well-calibrated Sun photometers that have been measuring AOD (with an accuracy of 0.01) and retrieving a set of particle properties around the globe (Holben et al., 2001).

2.2 CALIOP aerosol extinction profiles

CALIOP is a two-wavelength, polarization lidar onboard the Cloud-Aerosol Lidar and Infrared Pathfinder Satellite Observation (CALIPSO) satellite with an equator-crossing time of about 1:30 PM and 1:30 AM, and a 16-day repeat cycle. Since June 2006, CALIOP has been almost continuously collecting high vertical resolution (e.g., 30 m) profiles of the attenuated backscatter by aerosols and clouds at 532 nm and 1064 nm wavelengths along with polarized backscatter at 532 nm between 82ºN and 82ºS (Winker et al., 2009). Currently, CALIOP is the only spaceborne lidar on orbit that provides this key information about the vertical distribution of aerosol. The unprecedented long data record of CALIOP aerosol profiles accumulated over more than a decade has contributed to a revolutionary understanding of aerosols in the Earth system. It is worth noting that CALIOP can detect aerosol layers in clear sky, below thin cirrus clouds, and above opaque low-level clouds during both day and night, although the nighttime data have better accuracy than the daytime data (Winker et al., 2010). In this study, we will use the CALIOP version 4.20 aerosol extinction profile data at a nominal horizontal resolution of 5 km supplemented by the vertical feature masks in both daytime and nighttime, which represents significant improvements over the previous data versions (Kim et al., 2018). We only use high quality aerosol data with the Cloud Aerosol Discrimination (CAD) score between -100 and -90 following Yu et al. (2019).

2.3 SEVIRI dust RGB composite imagery

https://doi.org/10.5194/acp-2021-73
Preprint. Discussion started: 3 March 2021


Atmospheric Chemistry and Physics Discussions

SEVIRI onboard the Meteosat Second Generation (MSG) satellite series in geostationary orbit (36,000 km) and centered at (0ºN,0ºE) provides images of Europe and Africa at a frequency of every 15 min, day and night (Schmetz et al., 2002). This allows for monitoring the genesis and movement of dust clouds at high temporal resolution (Schepanski et al., 2007; Ashpole and Washington, 2012). The brightness temperature (BT) at 10.8 μm and two BT differences (between 8.7 μm and 10.8 μm, and between 12.0 μm and 10.8 μm) are rendered to red-green-blue (RGB) beams to highlight the presence of dust and different cloud phases (deep clouds, middle clouds, and low clouds) (Lensky and Rosenfeld, 2008; Brindley et al., 2012). In this study, we use SEVIRI RGB imagery to illustrate the genesis and movement of mesoscale convective systems, haboobs, and dust plumes from other sources.

2.4 PM concentrations from EPA air quality network

EPA of the United States has established a comprehensive network across the nation (including Puerto Rico, and the U. S. Virgin Islands) to monitor the outdoor air quality of ozone, PM, and other chemical species. In this study, we will use the measured daily $PM_{2.5}$ data in June 2020 over nine southern states of the U.S., including Florida, South Carolina, Georgia, Alabama, Mississippi, Louisiana, Arkansas, Oklahoma, and Texas. This wide swath of states captured the major influence of the massive dust intrusion on air quality. Unfortunately, most of EPA measuring sites in Puerto Rico were not active during the period of this study, except Canato where PM_{10} (PM with aerodynamic diameter of smaller than 10 μm) concentration was measured during the June 22-30 period. Given that in the southern U.S. the EPA network currently only collects PM_{10} concentration at very limited number of sites, our analysis will focus on $PM_{2.5}$.

2.5 GEOS simulations of aerosol

The NASA GEOS is a global Earth system model that includes components for atmospheric circulation and composition, ocean circulation and biogeochemistry, land surface processes, and data assimilation (Rienecker et al., 2011). The coupled atmospheric constituent module within the GEOS architecture most relevant to this study is an aerosol module based on the Goddard Chemistry Aerosol Radiation Transport (GOCART) model (Colarco et al., 2010). GOCART simulates major components of aerosols (with diameter between 0.02 and 20 μm) and some gaseous precursors, including dust, sea-salt, sulfate, nitrate, ammonium, organic carbon, black carbon, SO_2, dimethyl sulfide, and NH_3 (Chin et al., 2002, 2009, 2014; Ginoux et al., 2001; Bian et al., 2017). The model is run in a replay mode, with meteorological fields being taken from the Modern-Era Retrospective analysis for Research and Applications - version 2 (MERRA-2) reanalysis (Gelaro et al., 2017) every six hours. The model has a horizontal resolution of 1ºx1º and 72 layers in the vertical. The GEOS hourly outputs of aerosol are used in this study. Note that the model run does not assimilate satellite data of aerosol.

In the GOCART dust modeling, bulk dust emissions are calculated online based on 10-m wind speed and a pre-determined dust source function. The dust source function is a dynamic one that uses the topographic depression and the dynamic surface bareness derived from the satellite observations (Ginoux et al., 2001; Kim et al., 2013). This dynamic dust

https://doi.org/10.5194/acp-2021-73
Preprint. Discussion started: 3 March 2021


Atmospheric Chemistry and Physics Discussions

source function accounts for the seasonal and interannual variations of the surface bareness and soil moisture, which improves simulated temporal variation of dust aerosols over some semi-arid areas (Kim et al., 2013). Currently, dust particle size distribution (PSD) in GEOS model is described with five size bins (i.e., 0.2–2 μm, 2–3.6 μm, 3.6–6 μm, 6–12 μm, and 12–20 μm in diameter) (Ginoux et al., 2001; Chin et al., 2009). The size distribution of emitted dust is empirically prescribed following Tegen and Fung (1994). Emitted dust is transported by winds and removed from the atmosphere via gravitational settling, dry deposition by turbulence, and scavenging by large-scale and convective rain. The gravitational settling is calculated with an assumption of spherical particle following a method as described in Ginoux et al. (2001). The model parameterizes large-scale in-cloud and below-cloud scavenging as a function of rainfall production rate and precipitation fluxes, respectively, and the scavenging in convective updrafts as a function of the updraft mass flux. Dust optical properties in the model are based on the Meng et al. (2010) database that incorporates Mie, T-Matrix, DDA, and geometric optics (depending on size parameter), as described in Colarco et al. (2014). The shape distribution presently used is the spheroidal distribution proposed by Dubovik et al. (2006).

3 Results

3.1 Observational characterizations of the dust event

In this section we use satellite and ground-based observations to characterize the dust event, including the evolution of trans-Atlantic dust plumes, strength of the dust intrusion event in the context of last two decades, impacts of the dust intrusion event on air quality in Puerto Rico and the southern U.S., and synoptic meteorological conditions controlling the dust event.

3.1.1 Evolution of the trans-Atlantic dust plumes

Horizontal variations of trans-Atlantic dust plumes are characterized by MODIS aerosol retrievals. **Figure 2** shows the MODIS daily AOD maps from June 13 to 27 at a frequency of every other day (a full day-to-day variation of AOD can be seen in an animation in Supplementary Online Material). Here MODIS observations from both Terra and Aqua are combined to represent daily AOD with a better spatial coverage than either alone. Overlaid on the AOD map is horizontal wind vectors at about 4km altitude from the MERRA2 reanalysis. Clearly seen in these maps are the dust plumes of as wide as 2500 km (confined within 5ºN-30ºN latitude belt) being transported across the tropical Atlantic Ocean in a meandering path and ultimately reaching the Gulf of Mexico and the southern U.S. A discontinuity along the West African coastline reflects difference between the MODIS DT and DB algorithms. In the early days (June 13-15), the dust plume was largely confined to the African coastal region (east of 35ºW), which is consistent with the presence of a strong meridional wind component in the region. This coastal accumulation of dust led to a peak AOD of about 3.5 on June 17. Although the plume had already started moving westward on June 17 as a result of a much weakened meridional wind, the rapid ventilation of dust away of the African coast took place on June 18. On June 19, the plume extended from the African coast to 50ºW with more dust coming out of West African deserts. The dust

https://doi.org/10.5194/acp-2021-73
Preprint. Discussion started: 3 March 2021


Atmospheric Chemistry and Physics Discussions

plume front was swirling around a weak anticyclone with its front moving northward to nearly 30ºN. In the following days, the dust plume drifted south and reached the northern coast of South America on June 21. The plume with its front at 70ºW was followed by another narrow dust plume located near the coast of West Africa with AOD generally smaller than 1. It appears that significant dust in the plume had been deposited into the ocean during the period of June 19-21. Some new dust sources on were also evident over West Africa (e.g., southern Algeria, Mali, and Mauritania). On June 23 dual dust plumes appeared on the map, the primary "Godzilla" dust plume over the Caribbean Basin (centered around 15ºN and 68ºW) and the secondary dust plume near the African coast. The primary dust plume veered into the Gulf of Mexico in the direction of northwest on June 25, potentially striking a large swath of the southern US. While a branch of the dust plume appeared to enter the Florida panhandle, the plume structure off the gulf coast from Texas to Louisiana was not visible from MODIS due to the presence of clouds. Meanwhile the secondary dust plume was approaching the eastern Caribbean Sea at about 60ºW. On June 27, the secondary dust plume reached the Gulf of Mexico, but did not move toward the southern U.S. due to the dominant zonal winds in the Gulf region.

To track the progression of dust plumes across the tropical North Atlantic Ocean, we present MODIS daily AOD and FMF averaged over 5°N-30°N in the time-longitude Hovmöller diagrams, as shown in **Figure 3**. During the June 10-30, 2020 period, three distinct dust plumes stand out with high AOD and low FMF (dust particles are coarse and have smaller values of FMF than background marine aerosol and combustion aerosol). The most prominent dust plume, i.e., the Godzilla dust plume, started to build up along the African coast on June 13-15. Initially the dust plume was generally confined and accumulated to the coastal region east of 35°W. As such over the coastal water off West Africa, high AOD (1.5~2.0) and small FMF (0.1~0.2) persisted for several days. On June 17-18, the intense dust plume was transported westward rapidly by an African Easterly Wave, reaching the eastern Caribbean (at 60°W) on June 21 with AOD of 0.9-1.3 and FMF of about 0.2, and then the Gulf of Mexico (at 90°W) on June 25 with AOD of about 1.0 and FMF of 0.3. AOD did not undergo significant decrease from the eastern Caribbean to the Gulf of Mexico, which would yield a strong influence on the southern U.S. Additionally, two weaker but still notable dust plumes are also displayed in the Hovmöller diagrams. One plume started its trans-Atlantic journey from the coast of North Africa (at 15°W) with AOD of ~1.2 and FMF of ~0.1 on June 10. The AOD of this plume decreased rapidly to ~0.3 at 45°W on June 15. No clear plume can be seen beyond this point, suggesting that this dust plume had been quickly removed from the atmosphere and did not reach the Caribbean Basin. On the other hand, another dust plume originated at the coast on June 22 with a smaller AOD of about 0.9 was transported all the way to the Caribbean Basin and Gulf of Mexico. The plume reached the eastern Caribbean Basin (at 60°W) on June 26 and the Gulf of Mexico (at 90°W) on June 30.

Figure 4 shows the time series of MODIS and AERONET daily AOD from June 10 to June 30, 2020 at seven AERONET sites in West Africa and the Caribbean Basin, including Cape Verde, Tamanrasset, Ben Salem, Cape San Juan, La Parguera, Guadeloup, and Ragged Point. These comparisons show that MODIS retrievals well capture the time evolution of the dust events observed by AERONET sun photometers, in particular over the Caribbean Basin.

https://doi.org/10.5194/acp-2021-73
Preprint. Discussion started: 3 March 2021


Atmospheric Chemistry and Physics Discussions

The vertical structures of the dust plumes are characterized by CALIOP observations. **Figure 5** displays the CALIOP aerosol extinction curtains over West Africa (June 17), the African coast (June 18), and the Caribbean Basin (June 23 and 24). In West Africa and along the coast, the top of the dust plume is at 6-8 km, which is higher in the north than in the south. This dust plume top altitude is higher than the climatology of summertime extreme dust events (~5 km) (Huang et al., 2010). The intense dust layers stay above the low-level clouds (light grey shading) (Figures 5a and 5b). Also, the heavy dust layer attenuates the CALIOP beam entirely so that no signal (black shading) is apparent below 2 km in some locations (Figure 5b). After being transported to the Caribbean Basin, the top of the dust plume is at about 4 km and the dust layer appears to mix with marine aerosol in the boundary layer. The mixing leads to the maximum extinction near the surface. Because the aerosol loading was significantly reduced through deposition processes along the transport, totally attenuated features do not exist over the Caribbean Basin. The CALIOP high-resolution measurements also show fine structures in the dust plume, including several sandwiched layers of high aerosol extinction of greater than 0.5 km^{-1} between 1.5 km and 4 km near the African coast and about 0.3 km^{-1} between 1 and 3 km in the Caribbean Basin.

3.1.2 Impacts on air quality in Puerto Rico and the southern U.S.

As shown in Figure 2, the gigantic dust plume swept across Puerto Rico. During this dust event PM_{10} was sampled only at the EPA Catano site (18.43ºN, 66.14ºW) (**Figure 6a**). PM_{10} peaked on June 23, with the concentration of 453 μg m^{-3}. The PM_{10} concentration was also higher than the statistical average a day before (161 μg m^{-3} on June 22) and after (139 μg m^{-3} on June 24. On June 27 and 28, PM10 concentration was 95 and 91 μg m^{-3}, respectively, indicating the influence of the secondary dust plume discussed earlier. This day-to-day variation in PM_{10} concentration is different than AOD variation in Cape San Juan and La Parguera where AOD peaked on June 22 (Figure 4). This difference can be explained by the aerosol vertical distribution, as shown in Figure S1. Generally, the dust layer was elevated in altitude on June 22 but touched the ground on June 23 and 24, although CALIOP tracks were not always close to the surface site. By examining the PM_{10} data record since 1994 at Catano site, we identified 24 days with daily PM_{10} > 100 μg m^{-3} (Figure 6b). Clearly, June 23, 2020 had the highest PM_{10} in the whole record, while June 22 and 24 had the third and fifth highest PM_{10}, respectively.

The dust plume intruded into the southern U.S. through the Gulf of Mexico pathway, affecting PM levels and thus possibly air quality in the southern U.S. states. We examined daily $PM_{2.5}$ concentrations in June 2020 at all available EPA air quality sites (~150) in the nine southern U.S. states and found that the surface $PM_{2.5}$ concentrations at a number of sites were substantially elevated on June 26 and 27 in comparison to the days before and after. We categorized the $PM_{2.5}$ data into four ranges: <15, 15-35, 35-50, and >50 μg m^{-3} and marked with different colors, as illustrated in **Figure 7**. On June 26, 31 out of 158 sites (or 20%) observed $PM_{2.5}$ exceeding the EPA air quality standard of 35 μg m^{-3}. On June 27, 62 out of 150 sites (or 41%) exceeded the EPA standard. The maximum $PM_{2.5}$ concentration observed was 73.9 μg m^{-3} (St. Marks / Florida) and 73.5 μg m^{-3} (Eagle Pass / Texas) on June 26 and 27, respectively. Although only a few sites have PM_{10} concentration available,

https://doi.org/10.5194/acp-2021-73
Preprint. Discussion started: 3 March 2021


Atmospheric Chemistry and Physics Discussions

three sites observed PM_{10} greater than 100 μg m^{-3}, including 136 μg m^{-3} in North Tulsa / Oklahoma (June 27), 135 μg m^{-3} in Jackson NCORE / Mississippi (June 26), and 113 μg m^{-3} in OKC North / Oklahoma (June 27).

A notable feature in Figure 7 is that a number of sites in the Florida panhandle region detected $PM_{2.5}$ concentration > 50 μg m^{-3} for both days, although $PM_{2.5}$ concentrations remained low (<15 μg m^{-3}) in southern and central Florida. This suggests that the dust plume took the Gulf of Mexico pathway and affected the Gulf coast especially, which is corroborated by remote sensing measurements of dust plume intrusion to the region (**Figure 8**). The AERONET measurements at Tallahassee (illustrated in the inset of June 27 map) show maximum AOD of 1.47 on June 26, which is substantially higher than 0.1-0.2 during the June 10-23 period. Meanwhile the FMF on June 27 was 0.28, which represented a substantial drop from 0.82 on June 22. MODIS AOD around Tallahassee shows an increase from about 0.2 on June 24 to 0.5 and 0.8 on June 25 and26, respectively. On June 25, CALIOP also passed through the region with the aerosol extinction coefficient of 0.1-0.5 km^{-1} from surface to about 4 km. These measurements provide clear evidence that large amounts of dust did intrude into and degrade the air quality in the Panhandle region.

3.1.3 A historic event in the past two decades and its synoptic control

The June 2020 event of African dust intrusion into the Caribbean Basin and the Americas is a historic one projecting above the climatology from the past two decades, as registered in the MODIS/Terra data record since 2000 **(Figure 9)**. We carried out regional analysis of MODIS Terra daily AOD since 2000 in seven regions as defined in Figure 9a: Saharan deserts (SAHD), North African Coast (NAFC), the northeast coast of South America (NCSA), the southern Caribbean Basin (SCRB), the northern Caribbean Basin (NCRB), the Gulf of Mexico (GMEX), and the tropical eastern Pacific Ocean (TEPO). Results of the regional analysis are shown in Figure 9b-9h. In each region, daily AOD for January – June 2020 is marked as red dots and lines, with the evolution of daily AOD from June 10 to 30, 2020 being elaborated in the inset. For visual clarity, we present the 2000-2019 daily AOD climatology in the form of the 20-year average (black line) plus its range (grey vertical bar). Clearly, the dust event in June 2020 has the highest AOD over the past two decades over the North African coast (b), the southern Caribbean Basin (c), and the northern Caribbean Basin (d). In the northeast coast of South America (e), the dust transport to this region peaks in March-June with a minimum in August-November, which is determined by the seasonal migration of ITCZ (Yu et al., 2015a, 2015b; Prospero et al., 2014). Despite this, the 2020 June event had the second highest AOD over the past two decades and was the highest in June. The Gulf of Mexico (f) and the tropical eastern Pacific Ocean (g) are highly impacted by biomass burning smoke from the central America in spring. Although the June 2020 dust event had lower AOD than for some extreme springtime biomass burning events, it was indeed the highest in June. Moreover, it is very rare for African dust to make it into the tropical eastern Pacific because observations have suggested a Central American barrier to dust transport (Nowottnick et al., 2011). Therefore, for all these six regions affected by trans-Atlantic dust transport, the June 2020 dust is an historic event over the past two decades when seasonal variations of dust and smoke transport are factored in. On the contrary, the MODIS AOD over the Saharan deserts (h) does not indicate that daily dust emissions from North Africa

https://doi.org/10.5194/acp-2021-73
Preprint. Discussion started: 3 March 2021


Atmospheric Chemistry and Physics Discussions

were particularly large in early and mid-June. In fact, it was smaller than AOD in late May and June 6-8, 2020. Although the 2020 June AOD was higher than the climatological average in June, it was not the highest. An analysis in West Africa (10ºN-30ºN, 17ºW-10ºE), which is a part of the SAHD and likely the major source region for this dust event, displays similar AOD variations (see Figure S2).

Given that the dust loading in source regions in June 2020 were large albeit not historic (Figure 9h and Figure S2), the observed historic intrusion of African dust into the Caribbean Basin and the southern U.S. should have been modulated by meteorological conditions. The North Atlantic subtropical high (NASH), also known as the Bermuda-Azores high is a semi-persistent synoptic system that affects the meteorology and atmospheric circulations in West Africa and tropical Atlantic Ocean. The variation in NASH location and intensity would affect how the dust is transported across the tropical Atlantic Ocean. Here we analyze the MERRA2 meteorology associated with the dust episode by focusing on geopotential height and wind. **Figure 10** displays the evolving spatial patterns of the geopotential height and wind vectors at 600 hPa from June 14 to June 19. On June 14, the subtropical high was centered at (45ºW, 43ºN) with a maximum height of about 4500 m. This ridge system was accompanied by a low-pressure system or trough to its southeast around the Azores and an extensive high-pressure system (~4550 m) over West Africa. This setting of synoptic systems created an unfavorable atmospheric circulation condition for trans-Atlantic transport of dust. At the lower latitudes (south to ~20ºN), West Africa was dominated by strong northeasterly winds, which rapidly exported dust from Sahara-Sahel transit to the eastern Atlantic Ocean. But the easterly veered to the north in the coastal ocean (15ºW-35ºW), to the east at the northern fringe of the African continent (30ºN-35ºN), and eventually to the south in central Africa. This created a nearly closed atmospheric circulation system over West Africa and the eastern North Atlantic Ocean that could recirculate and trap the dust in the West African coast. The unfavorable synoptic systems persisted through June 15 and 16, although they were gradually weakened. By June 17-19, the subtropical high weakened further and drifted southward; meanwhile the trough over Azores was gradually filled up. The mid-latitude westerly pushed southward along the African coastline and broke up the closed atmospheric circulation over West Africa and the coastal ocean. As a result, dust outflow region was dominated by a strong African Easterly Jet (AEJ), which would favor the rapid transport of the accumulated dust from the African coast toward the Caribbean Basin.

Satellite observations corroborate the above analysis of the potential control of the synoptic systems on distributing African dust. As shown earlier in Figures 2 and 3, MODIS AOD started to build up on June 13 but a majority of the dust did not transport westward beyond the 35ºW until June 18. The highest AOD near the coast occurred on June 17. Moreover, the dust distribution modulated by the synoptic systems can be vividly displayed in an animation of SEVIRI full-disk RGB dust imageries once every 30 min over the June 12 -25 period (https://doi.org/10.5446/51548). Additionally, the animation in the SOM clearly shows the evolution of haboobs and their radial outflow behaviour, driven by outflows from convective downdrafts, which is not always evident in the still images. Here we show a sequence of SEVIRI still images (zoomed in North Africa) at 12Z of June 14-19, 2020 to illustrate the day-to-day evolution of the dust plumes (**Figure 11**). In these images, magenta, dark red, orange, and dull pink denotes dust, deep clouds, middle clouds, and low clouds, respectively. On June 14, SEVIRI detected two dust plumes (Figure 11a). One plume originating from the southern Mauritania was dispersed over a

https://doi.org/10.5194/acp-2021-73
Preprint. Discussion started: 3 March 2021


Atmospheric Chemistry and Physics Discussions

small coastal area (22ºW-16ºW and 12ºN-20ºN). The other dust plume was originated from a haboob developed over Niger due to strong downdrafts associated with a mesoscale convection system (dark red). The dust plume was situated north of the track of the convective system and was trailing the rapid moving deep clouds because of the much weaker wind speed than in the convective core (refer to Figure 10). The convective systems swept swiftly across West Africa and reached the coastal ocean by early hours of June 15. This formed an extensive dust belt between 15ºN-22ºN that extended from Niger to the coast of Mauritania, as shown in Figure 11b. The haboob-generated dust mixed with that produced from West African deserts and stayed over coastal water (east to 30ºW and 15ºN - 30ºN). The extensive dust belt continued to proceed towards the ocean on June 16 and more dust was accumulated into the coastal region (east to 40ºW, Figure 11c). These images clearly show that dust emerging from the continent accumulated over the coastal region for more than three days, yielding the heaviest dust plume on June 17. Then this amplified dust plume was ventilated out of the coastal region by the easterlies on June 18 and 19 (Figures 11e and 11f), leading to the historic intrusion of African dust into the Caribbean Basin and southern U.S. Note also that additional dust plumes from haboobs (June 18) and other West African sources (June 19) were added to the trans-Atlantic transport.

The above analysis suggests that the strength and location of NASH plays an important role in modulating the trans-Atlantic dust transport during this historic dust intrusion event. It is intriguing to compare the June 2020 NASH with other years. **Figure 12** compares the June geopotential height at 600 hPa between 2020 (a) and 1980-2019 climatology (b). Clearly, the NASH in June 2020 was stronger and located further north in comparison to the 40-year climatology. As shown in (c), the geopotential height in 2020 is more than 80 m higher than the climatology. South to this high anomaly is a low anomaly that extends from Bermuda to western Europe, with the lowest taking place off the coast of West Europe and the second lowest between Azores and Canary Islands. Over West Africa, the geopotential height in 2020 is higher than the climatology by up to 20 m over the northwestern Africa. Over the last four decades, the 2020 geopotential height over the high anomaly center (60ºW-30ºW, 35ºN-50ºN) is the second highest, slightly lower than 2006 (d). This analysis suggests that the subtropical high in June 2020 was highly anomalous in both the intensity and position.

3.2 GEOS model simulations of the dust intrusion event

In section 3.1, we have characterized the evolution of the historic dust plume in three dimensions associated with synoptic systems and assessed its impact on air quality in the southern U.S. by using a set of satellite and ground-based observations. Here we assess to what extent the GEOS model can reproduce the observed characteristics of this historic event. Similar to Figure 9, we analyze GEOS AOD from January 1, 2000 to June 30, 2020 on the regional basis (see Figure S3 in SOM). It shows that although the model characterizes the June 2020 event as a historic one over the North African coast (NAFC) and the southern Caribbean Basin (SCRB), the magnitude is more than a factor of 2 smaller than the MODIS AOD. Similar to the MODIS observations, the GEOS AOD over the desert (SAHD) during the event is not historically high. Unlike the MODIS observations, GEOS simulations of AOD over the other four regions are not the highest even after accounting for seasonal

https://doi.org/10.5194/acp-2021-73
Preprint. Discussion started: 3 March 2021


Atmospheric Chemistry and Physics Discussions

variations of dust and smoke transport. In the following, we further compare the GEOS simulations of aerosol three-dimensional distributions with MODIS and CALIOP observations over dust source region and along the trans-Atlantic transport route.

3.2.1 Dust source region

As discussed earlier and displayed in the SEVIRI animation, the major source of the Godzilla dust plume is associated with intense haboobs generated by a strong and fast-moving convective system over the southern Sahara from June 13 to June 15. How does the GEOS model perform in simulating haboobs associated with mesoscale convective systems? **Figure 13** shows an example comparing the GEOS modeling with MODIS and CALIOP observations on June 14. Clearly, GEOS (Figure 13b) underestimates MODIS AOD (Figure 13a) in Niger where the haboobs originated, although the GEOS AOD is higher than MODIS AOD near the coast. The GEOS simulated dust plume also drifts northwards over Mauritania, in comparison to the MODIS observation. There was a CALIPSO track passing through the convective system and associated dust haboob at 13:14Z (Figure 13c). CALIPSO observation shows that the dust extinction within the haboob is nearly uniform from the surface up to about 4 km (Figure 13d). In contrast, the GEOS model simulates the maximum aerosol extinction near the surface, which decreases by a factor of about 4 from the surface to 4 km altitude (Figure 13e).

A similar comparison for the June 15 case was displayed in **Figure 14**. On this day, the long-stretched dust plume extending from Niger to the African coast (Figure 14a) was a remanent of the haboobs from the previous day. Again, the GEOS model underestimates the AOD and simulates a plume transported northwards by about 800 km over Mali (Figure 14b), extending further north than the MODIS AOD observation. Although the top of the dust plume simulated by GEOS is largely consistent with the CALIOP observation, the vertical distribution of aerosol extinction within the plume is quite different. Although CALIOP reveals the elevated dust plume (either above clouds or totally attenuated features) with the highest extinction at the altitude of 4-6 km, the GEOS model displays a rapid decrease of aerosol extinction with increasing altitude.

Both comparisons confirm that the model with a horizontal resolution of one degree has a grand challenge to realistically simulate the mesoscale convection and haboobs. The model substantially underestimates dust loading over the desert, implying a very substantial underestimate of dust emissions. The model also drifts the dust plume northwards and fails to pump up dust from the surface to higher altitudes for ensuing long-range transport. These modeling deficiencies affect the simulation of trans-Atlantic dust transport as discussed in next section.

3.2.2 Trans-Atlantic dust transport

Figure 15 shows GEOS simulation of the evolving dust plume during the period of June 13-27, 2020, similar to the MODIS characterization as shown in Figure 2. A comparison of Figure 15 and Figure 2 shows that the model well reproduces the MODIS observed track of meandering dust plume carried by the wind systems, although the modeled plume center shifts northwards by about 2 degree. However, the model substantially underestimates the MODIS-observed AOD, which becomes

https://doi.org/10.5194/acp-2021-73
Preprint. Discussion started: 3 March 2021


Atmospheric Chemistry and Physics Discussions

more pronounced with increasing transport distance. To further quantify the difference between GEOS and MODIS, we create the Hovmöller diagrams for GEOS AOD and AOD difference between MODIS and GEOS (MODIS – GEOS), as shown in **Figure 16**. The GEOS AOD Hovmöller diagram clearly shows that the model reproduces the distinct trans-Atlantic dust plume tracks as observed by MODIS (Figure 3). However, the GEOS substantially underestimated the MODIS observations. For the primary or "Godzilla" dust plume, the MODIS AOD is higher by up to 1 (corresponding to a factor of 2) near the African coast and by up to 0.6 (corresponding to a factor of 5) in the Caribbean Basin than the model simulation. The increasing MODIS and GEOS discrepancy with increasing transport distance suggests that GEOS model removes the dust too efficiently from the atmosphere, consistent with previous finding (Yu et al., 2019; Kim et al., 2014). For the secondary dust plume with weaker intensity, the GEOS model performs better; generally, MODIS AOD is larger than GEOS AOD by a factor of no more than 2. A more complete view of MODIS and GEOS AOD evolution during June 10-30 period is displayed in an animation (https://av.tib.eu/media/50830). Finally, the long-term GEOS model simulations do not show that the Godzilla dust plume is historic over the past two decades.

The vertical structure of the "Godzilla" dust plume exhibits striking differences between GEOS and the CALIOP observations, as shown in **Figures 17 and 18**. The nine CALIPSO curtains are selected along the track of trans-Atlantic dust plume (Figure 3). GEOS hourly outputs closer to CALIOP overpass time are extracted along the CALIPSO track. While the along-CALIPSO track curtain plots in Figure 17 resolve the meridional and vertical distributions of the dust plume over the course of the trans-Atlantic transport, Figure 18 contrasts the differences between GEOS and CALIOP by averaging over the meridional extent (5ºN-30ºN) of the dust plume. When calculating average profiles, GEOS hourly outputs are sampled based on CALIOP observations of aerosol and clear-clean features only (that means the cloudy and fully attenuated features are excluded in averaging). Figures 17 and 18 collectively show several major discrepancies between CALIOP and GEOS. The GEOS model does not reproduce CALIOP-observed fine dust plume structure, presumably because of the model's coarse vertical resolution. East to the middle ridge of the tropical Atlantic Ocean (June 16-20), CALIOP observed an elevated dust layer of 1-2 km thick in the mid-troposphere with the extinction coefficient of greater than 0.4 km^{-1} and total attenuated layer just beneath the dust plume. This elevated dust plume descends continuously during the westward transport, with the peak aerosol extinction occurring at altitude of 4 km near the coast (15ºW) on June 16 to about 2 km on June 20 when entering the Caribbean at ~55ºW. This suggests that the dust plume travels westward at an average speed of 1000 km d^{-1} (~11.6 m s^{-1}) and descends at a rate of about 500 m d^{-1}(~20 m hr^{-1}), which agrees well with the climatology of the extreme dust events (Kaufman et al., 2005; Huang et al., 2010). GEOS model misses or substantially underestimates the elevated dust plume, although it generally agrees better with CALIOP at lower altitudes. During June 22 – 25 and in the west Atlantic Ocean and Caribbean Basin, the dust plume continues descending with distance, mixing with background marine aerosol in the boundary layer, and touches the surface. Compared to the tropical eastern Atlantic Ocean, the CALIOP-GEOS discrepancy becomes much larger in the lower atmosphere (Figure 18). When integrating aerosol extinction in the vertical column, the CALIOP to GEOS AOD ratio increases from 1.43 near the coast (June 16) to 1.84 in the middle ridge (June 20), and 3.46 in the Gulf of Mexico (June 25), suggesting that the CALIOP-GEOS discrepancy increases with distance. This feature is consistent with that between

https://doi.org/10.5194/acp-2021-73
Preprint. Discussion started: 3 March 2021


Atmospheric Chemistry and Physics Discussions

MODIS and GEOS as revealed and discussed earlier (Figure 16). The missing of the elevated dust layer by GEOS over the upwind ocean and desert regions contributes to the large discrepancies observed in the downwind regions as the dust plume descends. It is also possible that CALIOP observed high values of aerosol extinction in the lowest ~500 m layer may be prone to interference by surface signal and/or cloud contamination. When the lowest 500 m layer is excluded in the calculation of AOD, the CALIOP to GEOS AOD ratio ranges from 1.54 to 3.84, slightly larger than that for the whole column. Excluding the lowest 500 m layer does not reduce the discrepancy between CALIOP and GEOS.

4 Conclusions

We have used a set of remote sensing observations, including MODIS, CALIOP, SEVIRI, and AERONET, to characterize the three-dimensional evolution of the gigantic African dust intrusion into the Caribbean Basin and southern U.S. in late June 2020 (June 13-27, 2020). For this gigantic dust event the aerosol optical depth broke the MODIS record of the past two decades, with AOD more than 3.5 at the African coast and 1.8 in the Caribbean Basin. The dust plume, originating from the convectively generated haboobs over sources in West Africa (mainly Niger, Mali, and Mauritania), was lifted from the desert surface to altitudes of up to 6-8 km, which is higher than the 5 km for the climatological summertime extreme dust events (Huang et al., 2010). Due to the persistence of a closed atmospheric circulation system over West Africa, the large but not extreme daily dust loading from Sahara accumulated in the African coastal region (east to 35ºW) for about four days. The average transport speed of the dust plume is 1000 km d^{-1}, which agrees very well with the climatology of summertime extreme dust events (Kaufman et al., 2005; Huang et al., 2010). During trans-Atlantic transport the top of the dust plume descended from 6-8 km over the West African coast to about 4 km altitude over the Caribbean Basin and 2 km over the U.S. Gulf coast. The descent of dust plume imposes important implications for air quality in the Caribbean Basin and the southern U.S. In Puerto Rico, the Godzilla dust plume caused a record-breaking PM_{10} concentration of 453 μg m^{-3}. The dust intrusion into the southern U.S. raised the $PM_{2.5}$ concentration to a level exceeding the EPA air quality standard in about 20% and 40% of the EPA stations in nine southern states on June 26 and 27, respectively. The poorest air quality with $PM_{2.5}$ as high as 74 μg m^{-3} occurred in the Florida panhandle region and western Texas.

The analysis of MERRA2 meteorology suggests that the unfavorable ventilation condition and the resultant dust accumulation along the African coast in the early stage of the dust storm was associated with the anomalous strength and northward shift of the North Atlantic subtropical high (NASH) that was accompanied by the low-pressure system over the Azores and the high-pressure system over West Africa. In fact, June 2020 had the second strongest NASH over the past four decades, only slightly weaker than the 2006 record. When the NASH became weaker and wandered back to south, the dust outflow region was dominated by the African Easterly Jet (AEJ), which carried the accumulated dust plume rapidly and maintaining its high concentrations from the coastal region toward the Caribbean Basin within four days, resulting in the extraordinary dust loading observed. Our results do not fully agree with what Francis et al. (2020) found on the atmospheric drivers of the dust storm. For example, they argued that the development of a subtropical high off the coast of West Africa generated anomalously strong northeasterlies over Sahara (19º-30ºN, 20º-0ºW) that caused continuous dust emissions over

https://doi.org/10.5194/acp-2021-73
Preprint. Discussion started: 3 March 2021


Atmospheric Chemistry and Physics Discussions

four days and high dust loading in the eastern tropical Atlantic Ocean. Our analysis of the SEVIRI dust images showed that intense haboobs swept through Niger-Mali-Mauritania corridor (south of 20 º N generally) and contributed significantly to the dust event. The dust emissions associated with these haboobs cannot be adequately explained by the large-scale meteorology used in Francis et al. (2020), because the reanalysis cannot capture such strong winds accurately (Cowie et al., 2015; Roberts et al., 2017) and their focused dust source region is largely outside the corridor of the intense haboobs identified in the SEVIRI images. We also found that unique synoptic setting associated with anomalous NASH strength and position created the closed atmospheric circulations over West Africa and its adjacent coastal ocean for several days, which trapped the continuously emitted dust in the African coast. In addition, Francis et al. (2020) found that the AEJ was much strengthened by the anticyclonic circulation associated with the anomalous sub-tropical high, which favored a rapid westward transport of dust toward the Americas. However, our estimated trans-Atlantic transport speed of 1000 km d^{-1} is more or less the same as the speed for the summertime dust events during 2003-2007 (Huang et al., 2010), suggesting that the strong AEJ in June 2020 was unlikely to be a major factor for the highest-in-record dust detected in the Caribbean Basin.

In comparison to satellite observations, the GEOS model substantially underestimated dust loading over the desert, which were strongly related to emissions from haboobs. The model also did not lift up enough dust to the middle troposphere for ensuing long-range transport. These deficiencies are likely resulted from unrealistic representations of moist convection, haboobs, and the vertical transport of dust in the model, possibly related to the model's coarse horizontal and vertical resolutions. As a result, the model largely failed to capture the satellite-observed elevated dust plume along the cross-ocean track and underestimated the dust intrusion into the Caribbean Basin and the Americas by a factor of 4 or more for AOD. Nevertheless, the model reproduced the plume track reasonably well on a daily basis, suggesting that large-scale meteorological fields that drove the aerosol transport modeling are accurate. Assimilating satellite observations of aerosol optical depth into the model can significantly improve the model's prediction of column aerosol loading (Randles et al., 2017; Buchard et al., 2017). Given the substantial differences in the aerosol vertical distribution between GEOS and CALIOP, however, if the assimilation only normalizes the modeled vertical distribution by the column AOD, the assimilation will continue to put too much of the dust in the lower layers. This may continue to artificially enhance the dust deposition along the transport path and introduce high bias in the surface dust concentration, which is of concern for air quality applications. Modeling improvement needs to focus on developing more realistic representations of moist convections, haboobs, and the vertical transport of dust (e.g., Roberts et al., 2018).

This work demonstrates that haboobs and convective systems over Africa have the ability to impact conditions far downstream. It is vital that models possess a capability of simulating convective outflows driving dust uplift, followed by accurately redistributing this emitted dust vertically throughout the Saharan boundary layer up to ~6-8 km as the haboobs decay. This study shows that if models are not able to represent dust up to the high observed altitudes over source regions, the resulting long-range transport will be incorrect. O'Sullivan et al. (2020) recently found that modelled summertime dust in the tropical Eastern Atlantic region was too low in the atmosphere compared to in-situ aircraft observations and that part of the problem was that the coarser dust particles were both not lifted to high enough altitudes and also settled out of the atmosphere

https://doi.org/10.5194/acp-2021-73
Preprint. Discussion started: 3 March 2021


Atmospheric Chemistry and Physics Discussions

too rapidly. It is clear that in order to improve dust models' ability to represent dust transport, efforts are needed to improve the representation of processes controlling dust uplift (such as haboobs), dust redistribution through the Saharan boundary layer and processes controlling their emission, transport and deposition, as a function of size. It is vital that future evaluations incorporate observations of vertical distribution of dust in order to fully understand and evaluate dust models.

Data availability

All datasets of aerosol and meteorology were obtained from a variety of sources with public access: The MODIS aerosol data were obtained from the NASA Level-1 and Atmosphere Archive and Distribution System (LAADS) webpage (https://ladsweb.nascom.nasa.gov/). The CALIOP aerosol products were obtained from NASA Langley Research Center Atmospheric Science Data Center (https://eosweb.larc.nasa.gov/). SEVIRI RGB images were produced by Yaswant Pradhan of the Met Office and are provided in the supplementary. EPA $PM_{2.5}$ and PM_{10} data were downloaded from https://www.epa.gov/outdoor-air-quality-data/download-daily-data. MERRA-2 data are available at **MDISC**, managed by the NASA Goddard Earth Sciences (GES) Data and Information Services Center (DISC). The AERONET data were downloaded from https://aeronet.gsfc.nasa.gov/cgi-bin/webtool_aod_v3.

Supplements

Supplementary figures referred in the paper are provided online.

Author Contributions

HY and MC conceived the study. HY, QT, LZ, QS, YS, and DK analyzed satellite and surface observations as well as model outputs. YZ and RCL produced the MODIS enhanced dust retrievals for the event. HB performed the GEOS simulations. YP and CLR provided SEVIRI dust imagery. All co-authors participated in discussion of the analysis. The paper was written by HY and commented and revised by all co-authors.

Competing interests

The authors declare that they have no conflict of interest.

Acknowledgements

This work was supported by the National Aeronautics and Space Administration's (NASA) the Science of Terra, Aqua and Suomi-National Polar-orbiting Partnership program and the CALIPSO/CloudSat Science Team program administered by Dr. Hal Maring and Dr. David Considine, respectively. OMB acknowledges support from NASA ROSES #80NSSC19K0194. We thank the NASA Center for Climate Simulation for their support of the GEOS model simulation.

References

Ashpole, I, and Washington, R.: An automated dust detection using SEVIRI: A multi-year climatology of summertime dustiness in the central and western Sahara, *J. Geophys. Res., 117,* D08202, https://doi.org/10.1029/2011JD016845, 2012.

Bian, H., Chin, M., Hauglustaine, D. A., Schulz, M., Myhre, G., Bauer, S. E., Lund, M. T., et al.: Investigation of global particulate nitrate from the AeroCom phase III experiment. *Atmos. Chem. Phys., 17 (21),* 12911-12940, doi:10.5194/acp-17-12911-2017, 2017.

Brindley, H. E., Knippertz, P., Ryder, C., Ashpole, I.: A critical evaluation of the ability of the Spinning Enhanced Visible and InfraRed Imager (SEVIRI) thermal infrared red-green-blue rendering to identify dust events: Theoretical analysis, *J. Geosphys. Res., 117,* D07201, https://doi.org/10.1029/2011JD017326, 2012.

Buchard, V., Randles, C. A., da Silva, A. M., Darmenov, A., Colarco, P. R., Govindaraju, R., Ferrare, R., et al.: The MERRA-2 aerosol reanalysis, 1980 onward. Part II: Evaluation and case studies, *J. Climate, 30,* 6851-6872, doi:10.1175/JCLI-D-16-06013.1, 2017.

Carlson, T., Prospero, J. M.: The Large-Scale Movement of Saharan Air Outbreaks over the Northern Equatorial Atlantic, *Journal of Applied Meteorology, 11(2)*, 283-297. DOI:10.1175/1520-0450(1972)011<0283:TLSMOS>2.0.CO;2, 1972.

Chin, M., Ginoux, P., Kinnes, S., Torres, O., Holben, B. N., Duncan, B. N., Martin, R. V., et al.: Tropospheric aerosol optical thickness from the GOCART model and comparisons with satellite and sun photometer measurements, *J. Atmos. Sci., 59,* 461–483, 2002.

Chin, M., Diehl, T., Ginoux, P., and Malm, W.: Intercontinental transport of pollution and dust aerosols: Implications for regional air quality, *Atmos. Chem. Phys., 7,* 9013-9051, 2007.

Chin, M., Diehl, T., Dubovik, O., Eck, T. F., Holben, B. N., Sinyuk, A., and Streets, D. G.: Light absorption by pollution, dust and biomass burning aerosols: A global model study and evaluation with AERONET data, *Ann. Geophys., 27*, 3439-3464, 2009.

Chin, M., Diehl, T., Tan, Q., Prospero, J. M., Kahn, R. A., Remer, L. A., Yu, H., et al.: Multi-decadal aerosol variations from 1980 to 2009: a perspective from observations and a global model, *Atmos. Chem. Phys., 14,* 3657-3690, 2014.

Colarco, P., da Silva, A. M., Chin, M., and Diehl, T.: On-line simulations of global aerosol distributions in the NASA GEOS-4 model and comparisons to satellite and ground-based aerosol optical depth. *J. Geophys. Res., 115,* D14207, 2010.

Colarco, P., Nowottnick, E., Randles, C. A., Yi, B., Yang, P., Kim, K., Smith, J., Bardeen, C.: Impact of radiatively interactive dust aerosols in the NASA GEOS-5 climate model: Sensitivity to dust particle shape and refractive index, *Journal of Geophysical Research-Atmospheres 119(2),* 753-786. https://dx.doi.org/10.1002/2013jd020046, 2014.

Cowie, S. M., Marsham, J. H., Knippertz, P.: The importance of rare, high-wind events for dust uplift in North Africa, *Geophys. Res. Lett., 42,* 8208-8215, doi:10.1002/2015GL065819.

DeMott, P. J., Sassen, K., Poellot, M. R., Baumgardner, D., Rogers, D. C., Brooks, S. D., Prenni, A. J., and Kreidenweis, S. M.: African dust aerosols as atmospheric ice nuclei, *Geophys. Res. Lett., 30(14),* 1732, doi:10.1029/2003GL017410, 2003.

Dubovik, O., Sinyuk, A., Lapyonok, T., Holben, B. N., Mishchenko, M. I., Yang, P., Eck, T. F., et al.,:Application of spheroid models to account for aerosol particle nonsphericity in remote sensing of desert dust, *J. Geophys. Res. – Atmos., 111,* D11208, doi:10.1029/2005JD006619, 2006.

Engelstaedter, S., Washington, R., Flamant, C., Parker, D. J., Allen, C. J. T., Todd, M. C.: The Saharan heat low and moisture transport pathways in the central Sahara—Multiaircraft observations and Africa-LAM evaluation, *J. Geophys. Res. Atmos., 120,* 4417-4442, doi:10.1002/2015JD023123, 2006.

Evan, A. T., Foltz, G. R., Zhang, D., and Vimont, D. J.: Influence of African dust on ocean-atmosphere variability in the tropical Atlantic, *Nature Geosci., 4,* 762-765, 2011.

Francis, D., Fonseca, R., Nelli, N., Cuesta, J., Weston, M., Evan, A., and Temimi, M.:The atmospheric drivers of the major Saharan dust storm in June 2020, *Geophys. Res. Lett.,* 47, e2020GL090102. https://doi.org/10.1029/2020GL090102, 2020.

Gelaro, R., McCarty, W., Suarez, M. J., Todling, R., Molod, A., Takacs, L., Randles, C. A., et al.: The Modern-Era Retrospective Analysis for Research and Application, Version 2 (MERRA-2), *J. Climate, 30,* 5419–5454, 2017.

Ginoux, P., Chin, M., Tegen, I., Prospero, J., Holben, B. N., Dubovik, O., and Lin, S.-J.: Sources and global distributions of dust aerosols simulated with the GOCART model, *J. Geophys. Res., 106,* 20,255-20,273, 2001.

Holben, B. N., Tanre, D., Smirnov, A., Eck, T. F., Slutsker, I., Abuhassan, N., Newcomb, W. W., et al.: An emerging ground-based aerosol climatology: aerosol optical depth from AERONET, *J. Geophys. Res. - Atmos., 106 (11)*, 12067-12097, 2001.

Hsu, N. C., Jeong, M. J., Bettenhausen, C., Sayer, A. M., Hansell, R., Seftor, C. S., Huang, J., and Tsay, S. C., Enhanced Deep Blue Aerosol Retrieval Algorithm: The Second Generation. *J. Geophys. Res. – Atmos., 118 (16),* 9296–9315, 2013.

Huang, J., Zhang, C., and Prospero, J. M.: African dust outbreaks: A satellite perspective of temporal and spatial variability over the tropical Atlantic Ocean, *J. Geophys. Res., 115*, D05202, doi:10.1029/2009JD012516, 2010.

Jickells, T. D., An, Z. S., Andersen, K. K., Baker, A. R., Bergametti, G., Brooks, N., Cao, J. J., et al., Global iron connections between desert dust, ocean biogeochemistry, and climate, *Science, 308,* 67-71, doi:10.1126/science.1105959, 2005.

570 Karyampudi, V. M., Palm, S. P., Reagen, J. A., Fang, H., Grant, W. B., Hoff, R. M., Moulin, C., et al.: Validation of the Saharan Dust Plume Conceptual Model Using Lidar, Meteosat, and ECMWF Data, *Bulletin of the American Meteorological Society, 80(6),* 1045-1076. https://doi.org/10.1175/1520-0477(1999)080<1045:VOTSDP>2.0.CO;2, 1999.

Kaufman, Y. J., Koren, I., Remer, L. A., Tanre, D., Ginoux, P., and Fan, S.: Dust transport and deposition observed from the Terra-Moderate Resolution Imaging Spectroradiometer (MODIS) spacecraft over the Atlantic Ocean, *J. Geophys. Res. – Atmos., 110,* D10S12, doi:10.1029/2003JD004436, 2005.

Kim, D., Chin, M., Bian, H., Tan, Q., Brown, M. E., Zheng, T., You, R., et al.: The effect of the dynamic surface bareness to dust source function, emission, and distribution, *J. Geophys. Res., 118,* 1–16, doi:10.1029/2012JD017907, 2013.

Kim, D., Chin, M., Yu, H., Diehl, T., Tan, Q., Kahn, R. A., Tsigaridis, K., et al.: Sources, sinks, and transatlantic transport of North African dust aerosol: A multimodel analysis and comparison with remote sensing data, *J. Geophys. Res. – Atmos., 119,* 6259-6277, doi:10.1002/2013JD021099, 2014.

Kim, M., Omar, A., H., Tackett, J. L., Vaughan, M. A., Winker, D. M., Trepte, C. R., Hu, Y., et al.: The CALIPSO version 4 automated aerosol classification and lidar ratio selection algorithm, *Atmos. Meas. Tech., 11,* 6107-6135, 2018.

Lensky, I. M., and Rosenfeld, D.: Clouds-Aerosol-Precipitation Satellite Analysis Tool (CAPSAT), Atmos. Chem. Phys., 8, 6739-6753, https://doi.org/10.5194/acp-8-6739-2008, 2008.

Levy, R. C., Mattoo, S., Munchak, L. A., Remer, L. A., Sayer, A. M., and Hsu, N.: The Collection 6 MODIS aerosol products over land and ocean, *Atmos. Meas. Tech., 6,* 2989-3034, 2013.

Marshak, A., Herman, J., Szabo, A., Blank, K., Carn, S., Cede, A., Geogdzhayev, I., et al.: Earth Observations from DSCOVR/EPIC Instrument. *Bull. Am. Meteorol. Soc., 99,* 1829-1830, doi:10.1175/bams-d-17-0223.1, 2018.

Marsham, J. H., Hobby, M., Allen, C. J. T., Banks, J. R., Brocks, B. J., Cavazos-Guerra, C., Engelstaedter, S., et al.: Meteorology and dust in the central Sahara: Observations from Fennec supersite-1 during the June 2011 Intensive Observation Period, *J. Geophys. Res., 118,* 4069-4089, doi:10.1002/jgrd.50211, 2013.

Marsham, J. H., and Ryder, C. L.: Weather Insight - dust storms and haboobs, *Weather,* submitted, 2021.

Meng, Z., Yang, P., Kattawar, G., Bi, L., Liou, K., Laszlo, I.: Single-scattering properties of tri-axial ellipsoidal mineral dust aerosols: A database for application to radiative transfer calculations, *Journal of Aerosol Science, 41(5),* 501-512. https://dx.doi.org/10.1016/j.jaerosci.2010.02.008, 2010.

Miller, R. L., Tegen, I., and Perlwitz, J.: Surface radiative forcing by soil dust aerosols and the hydrological cycle, *J. Geophys. Res. – Atmos., 109,* D04203, doi:10.1029/2003JD004085, 2004.

Muhs, D. R., Budhan, J. R., Prospero, J. M., and Carey, S. N.: Geochemical evidence for African dust inputs to soils of western Atlantic islands: Barbados, the Bahamas, and Florida, J. *Geophys. Res., 112,* F02009, doi:10.1029/2005JF000445, 2007.

Nowottnick, E., Colarco, P., da Silva, A., Hlavka, D., and McGill, M.: The fate of Saharan dust across the Atlantic and implications for a central American dust barrier, *Atmos. Chem. Phys., 11,* 8415-8431, https://doi.org/10.5194/acp-11-8415-2011, 2011.

Okin, G. S., Mahowald, N., Chadwick, O. A., Artaxo, P.: Impact of desert dust on the biogeochemistry of phosphorus in terrestrial ecosystems, *Global Biogeochemical Cycles, 18,* GB2005, doi:10.1029/2003GB002145, 2004.

O'Sullivan, D., Mareno, F., Ryder, C. L., Pradhan, Y., Kipling, Z., Johnson, B., Benedetti, A., et al.: Modeling transport Saharan dust too low in the atmosphere: a comparison of the MetUM and CAMS forecast with observations, *Atmos. Chem. Phys., 20,* 12955-12982, https://doi.org/10.5194/acp-20-12955-2020, 2020.

Prospero, J. M.: Long-range transport of mineral dust in the global atmosphere: Impact of African dust on the environment of the southeastern United States, *Proc. Natl. Acad. Sci. U.S.A., 96,* 3396-3403, 1999.

Prospero, J. M., and Lamb, P. J.: African droughts and dust transport to the Caribbean: Climate change implications, *Science, 302,* 1024-1027, 2003.

Prospero, J. M., Collard, F.-X., Molinie, J. & Jeannot, A.: Characterizing the annual cycle of African dust transport to the Caribbean Basin and South America and its impact on air quality and the environment, *Global Biogeochem. Cycles, 29,* 757–773, doi:10.1002/2013GB004802, 2014.

Randles, C. A., da Silva, A. M., Buchard, V., Colarco, P. R., Darmenov, A., Govindaraju, R., Smirnov, A., et al.: The MERRA-2 aerosol reanalysis, 1980 onward, Part I: System description and data assimilation evaluation. *J. Climate, 30,* 6823–6850, doi:10.1175/JCLI-D-16-0609.1, 2017.

Remer, L. A., Kaufman, Y. J., Tanre, D., Mattoo, S., Chu, D. A., Martins, J. V., Li, R.-R., et al.: The MODIS aerosol algorithm, products, and validation, *J. Atmos. Sci., 62,* 947– 973, 2005.

Remer, L. A., Levy, R. C., Mattoo, S, Tanré, D., Gupta, P., Shi, Y., Sawyer, V., et al.: The Dark Target Algorithm for Observing the Global Aerosol System: Past, Present, and Future. *Remote Sensing, 12(18),* 2900; https://doi.org/10.3390/rs12182900, 2020.

Rienecker, M. M., Suarez, M. J., Gelaro, R., Todling, R., Bacmeister, J., Liu, R., Bosilovich, M. G., et al.: MERRA: NASA's Modern-Era Retrospective Analysis for Research and Applications, *J. Climate, 24,* 3624–3648, 2011.

Roberts, A. J., Marsham, J. H., Knippertz, P., Parker, D. J., Bart, M., Garcia-Carreras, L., Hobby, M., et al.: New Saharan wind observations reveal substantial biases in analysed dust-generating winds, *Atmos. Sci. Let., 18,* 366-372, 2017.

Roberts, A. J., Woodage, M. J., Marsham, J. H., Highwood, E. J., Ryder, C. L., McGinty, W., Wilson, S., et al.: Can explicit convection improve modelled dust in summertime West Africa? *Atmos. Chem. Phys., 18,* 9025-9048, https://doi.org/10.5194/acp-18-9025-2018, 2018.

Ryder, C. L., McQuaid, J. B., Flamant, C., Rosenberg, P. D., Washington, R., Brindley, H. E., Highwood, E. J., et al.: Advances in understanding mineral dust and boundary layer processes over the Sahara from Fennec aircraft observations, *Atmos. Chem. Phys., 15,* 8479-8520, https://doi.org/10.5194/acp-15-8479-2015, 2015.

Schepanski, K., Tegen, I., Laurent, B., Heinold, B., and Macke, A.: A new Saharan dust source activation frequency map derived from MSG-SEVIRI IR channels, *Geophys. Res. Lett., 34,* L18803, https://doi.org/10.1029/2007GL030168, 2007.

Schmetz, J., Pili, P., Tjemkes, S., Just, D., Kerkmann, J., Rota, S., and Ratier, A.: An introduction to Meteosat Second Generation (MSG), *B. Am. Meteorol. Soc., 83,* 977-992, 2002.

Song, Q., Zhang, Z., Yu, H., Kato, S., Yang, P., Colarco, P., Remer, L. A., and Ryder, C. L.: Net radiative effects of dust in tropical North Atlantic based on integrated satellite observations and in situ measurements, *Atmos. Chem. Phys., 18,* 11303-11322, 2018.

Swap, R., M. Garstang, S. Greco, R. Talbot, and P. Kallbert: Saharan dust in the Amazon Basin, *Tellus, Ser. B, 44,* 133-149, 1992.

Tao, Z., Braun, S. A., Shi, J. J., Chin, M., Kim, D., Matsui, T., and Peters-Lidard, C. D.: Microphysics and Radiation Effect of Dust on Saharan Air Layer: An HS3 Case Study. *Mon. Wea. Rev., 146 (6):* 1813-1835 https://doi.org/10.1175/mwr-d-17-0279.1, 2018.

Tegen, I. and Fung, I.: Modeling of mineral dust in the atmosphere: Sources, transport, and optical thickness, J. *Geophys. Res. – Atmos., 99,* 22897-22914, 1994.

Winker, D., Vaughan, M. A., Omar, A. H., Hu, Y., Powell, K. A., Liu, Z., Hunt, W. H., et al.: Overview of the CALIPSO mission and CALIOP data processing algorithms, *J. Atmos. Oceanic Technol., 26,* 2310-2323. https://doi.org/10.1175/2009JTECHA1281.1, 2009.

Winker, D. M., Pelon, J., Coakley Jr., J. A., Ackerman, S. A., Charlson., R. J., Colarco, P. R., Flamant, P., et al.: The CALIPSO Mission: A Global 3D View of Aerosols and Clouds. *Bull. Amer. Meteor. Soc., 91,* 1211–1229, 2010.

Winker, D. M., Tackett, J. L., Getzewich, B. J., Liu, Z., Vaughan, M. A., and Rogers, R. R.: The global 3-D distribution of tropospheric aerosols as characterized by CALIOP, *Atmos. Chem. Phys., 13,* 3345-3361, doi:10.5194/acp-13-3345-2013, 2013.

Yu, H., Remer, L. A., Chin, M., Bian, H., Tan, Q., Yuan, T., and Zhang, Y.: Aerosols from overseas rival domestic emissions over North America. *Science, 337,* 566–569, 2012.

Yu, H., Remer, L. A., Kahn, R. A., Chin, M., and Zhang, Y.: Satellite perspective of aerosol intercontinental transport: from qualitative tracking to quantitative characterization, *Atmos. Res., 124,* 73-100, 2013.

Yu, H., & Zhang, Z.: New Directions: Emerging satellite observations of above-cloud aerosols and direct radiative forcing, *Atmos. Environ., 72,* 36-40, 2013.

Yu, H., Chin, M., Yuan, T. L., Bian, H., Remer, L. A., Prospero, J. M., Omar, A., et al.: The fertilizing role of African dust in the Amazon rainforest: A first multiyear assessment based on CALIPSO lidar observations. *Geophys. Res. Lett., 42,*1984-1991 doi:10.1002/2015GL063040, 2015a.

Yu, H., Chin, M., Bian, H., Yuan, T., Prospero, J. M., Omar, A. H., Remer, et al.: Quantification of trans-Atlantic dust transport from seven-year (2007-2013) record of CALIPSO lidar measurements, *Remote Sens. Environ., 159,* 232-249, doi:10.1016/j.rse.2014.12.010, 2015b.

Yu, H., Tan, Q., Chin, M., Remer, L. A., Kahn, R. A., Bian, H., Kim, D., et al.: Estimates of African dust deposition along the trans-Atlantic transit using the decade-long record of aerosol measurements from CALIOP, MODIS, MISR, and IASI, *J. Geophys. Res. -Atmos., 124,* 7975-7996, 2019. https://doi.org/10.1029/2019JD030574.

Yuan, T. L., Oreopoulos, L., Zelinka, M., Yu, H., Norris, J., Chin, M., Platnick, S. E., et al.: Positive low cloud and dust feedbacks amplify tropical North Atlantic multidecadal oscillation. *Geophys. Res. Lett., 43 (3),* 1349–1356 doi:10.1002/2016gl067679, 2016.

Zhou, Y., Levy, R. C., Remer, L. A. Mattoo, S., and Espinosa, W. R.: Dust aerosol retrieval over the oceans with the MODIS/VIIRS dark-target algorithm: 1. Dust detection, *Earth and Space Science, 7,* e2020EA001221, https://doi.org/10.1029/2020EA001221, 2020.

Zhou, Y., Levy, R. C., Remer, L. A., Mattoo, S., Shi, Y., and Wang, C: Dust aerosol retrieval over the oceans with the MODIS/VIIRS dark-target algorithm: 2. Nonspherical dust model, *Earth and Space Science, 7,* e2020EA001222, https://doi.org/10.0129/2020EA001222, 2020.

https://doi.org/10.5194/acp-2021-73
Preprint. Discussion started: 3 March 2021

Atmospheric Chemistry and Physics Discussions

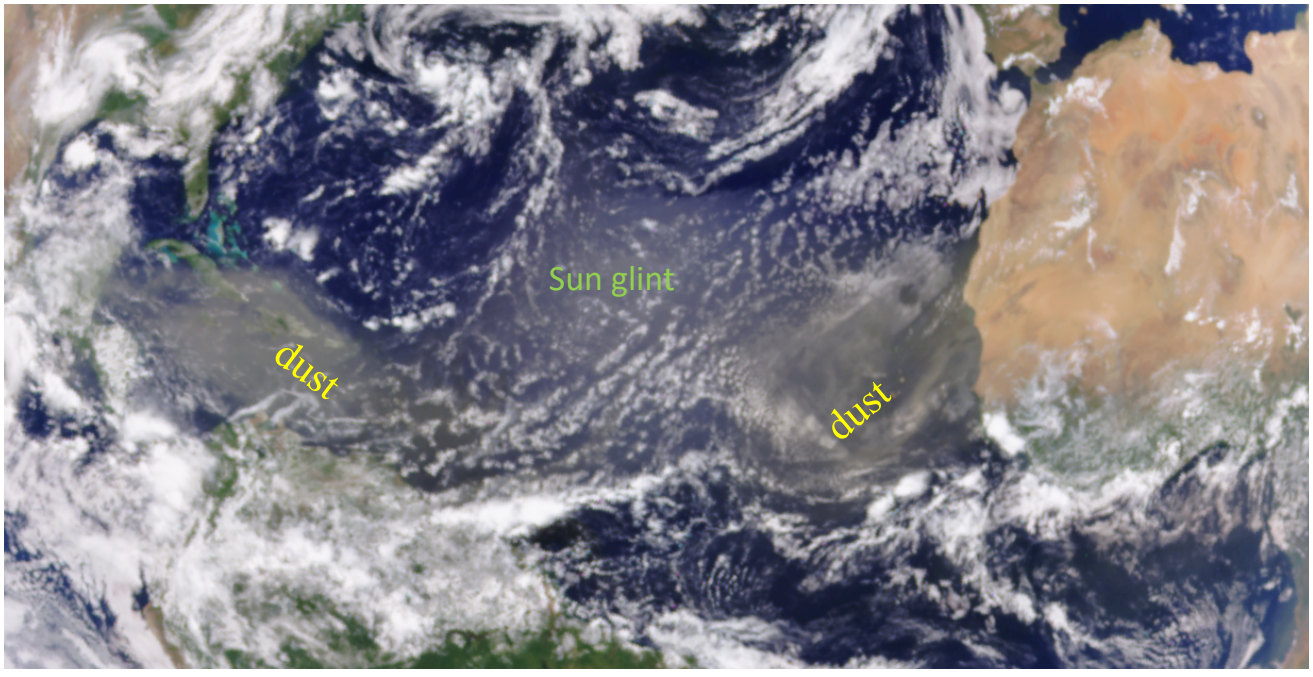

Figure 1: A panorama of dual dust plumes from one and a half million miles above the Earth's surface snapped by the EPIC/DSCOVR at 14:47:32 GMT on June 23, 2020 (https://epic.gsfc.nasa.gov).

685

https://doi.org/10.5194/acp-2021-73
Preprint. Discussion started: 3 March 2021

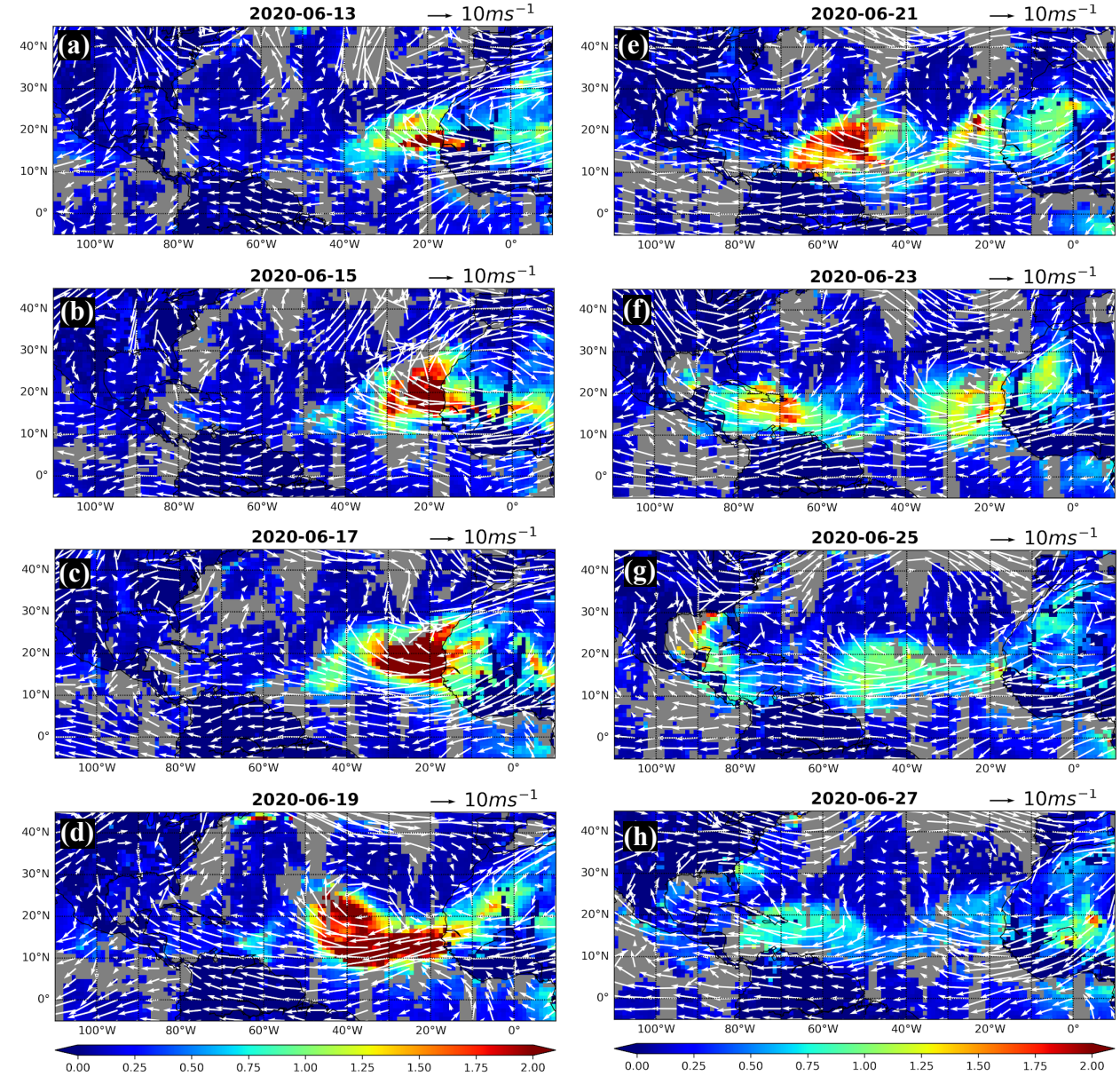

Figure 2: Evolution of dust plumes as revealed by MODIS AOD (color map) from June 13 to June 27, 2020. Overlaid on the AOD is the MERRA2 wind vectors at about 4 km altitude, which illustrates how the dust plumes are carried by atmospheric circulations from the coast of North Africa to the Caribbean Basin and the southern U.S. Gray areas indicate MODIS data gaps due to the presence of clouds or other unfavorable conditions for the retrieval.

https://doi.org/10.5194/acp-2021-73
Preprint. Discussion started: 3 March 2021

Atmospheric Chemistry and Physics Discussions

690

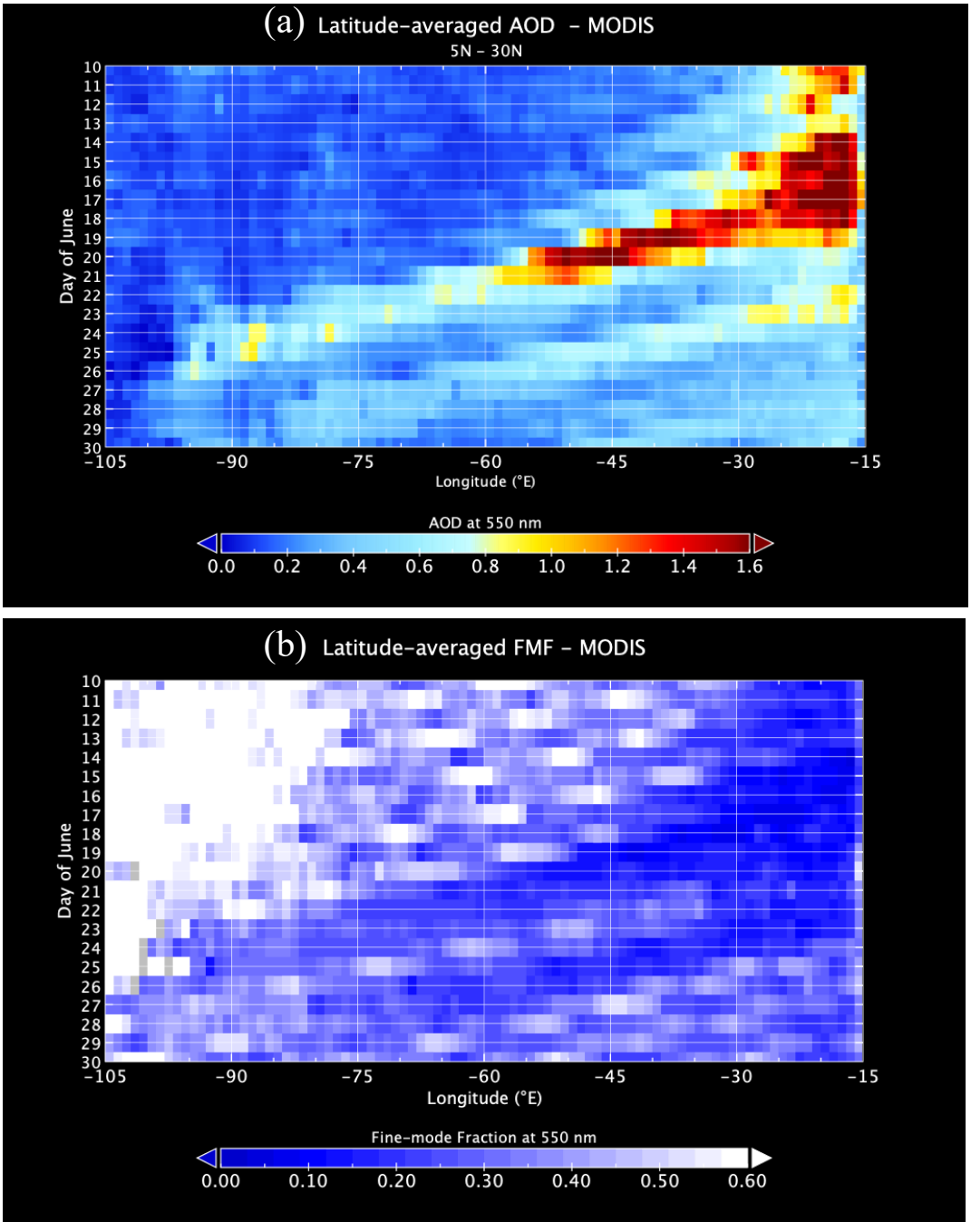

Figure 3: Tracks of trans-Atlantic dust plumes during June 10-30, 2020 as revealed in the longitude-time Hovmöller diagrams of MODIS daily AOD (top) and FMF (bottom). AOD and FMF are averaged over 5°N - 30°N.

https://doi.org/10.5194/acp-2021-73
Preprint. Discussion started: 3 March 2021

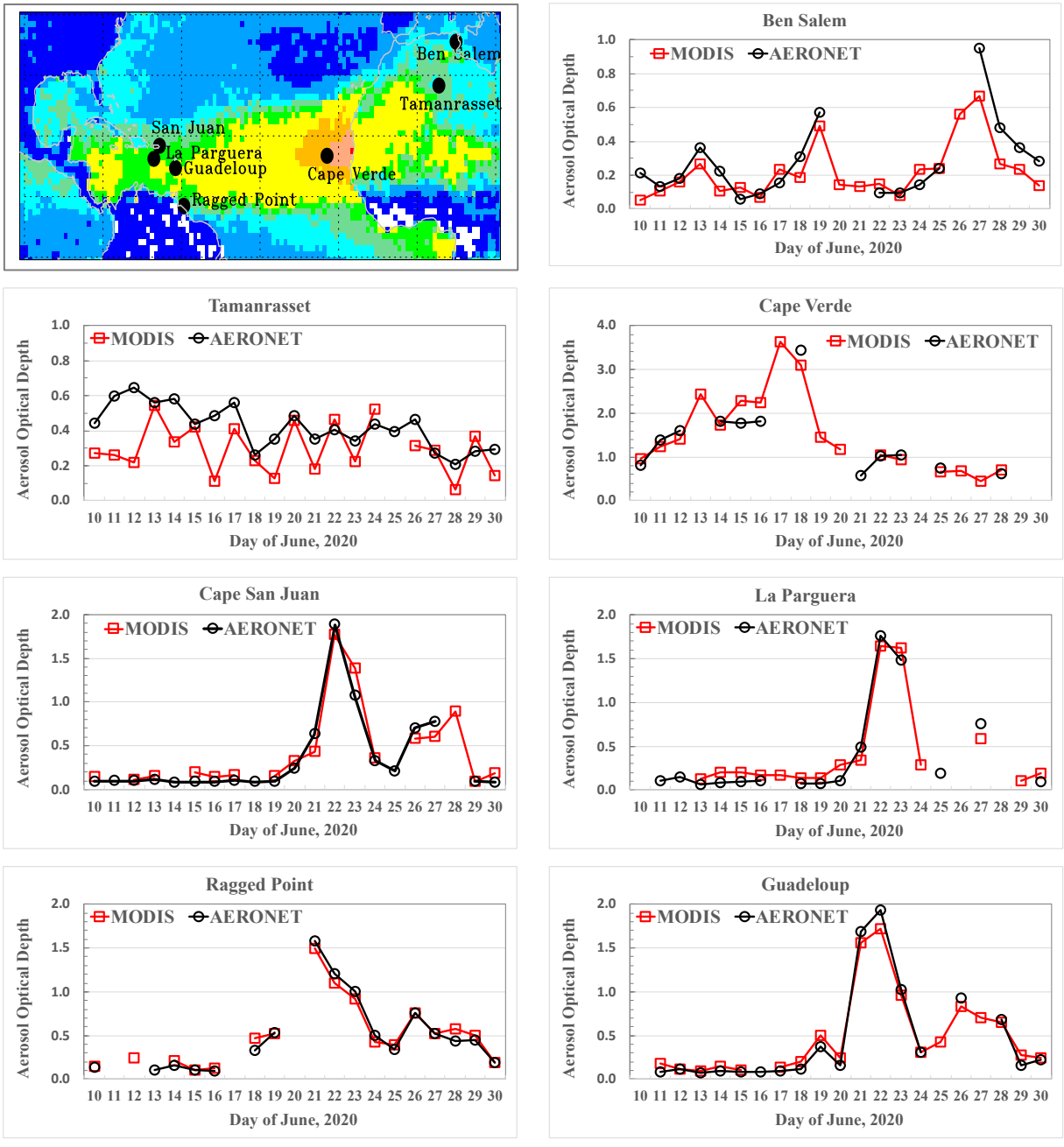

Figure 4: Time series of MODIS and AERONET daily AOD at 550 nm in seven AERONET sites from June 10 to 30, 2020.

https://doi.org/10.5194/acp-2021-73
Preprint. Discussion started: 3 March 2021

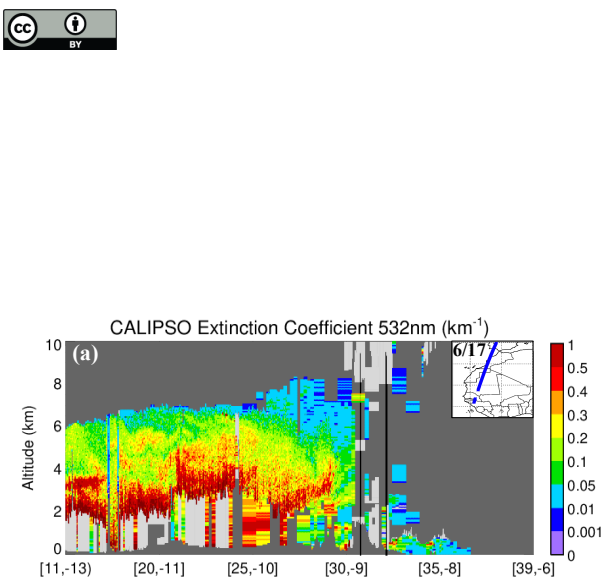

Atmospheric Chemistry and Physics Discussions

695

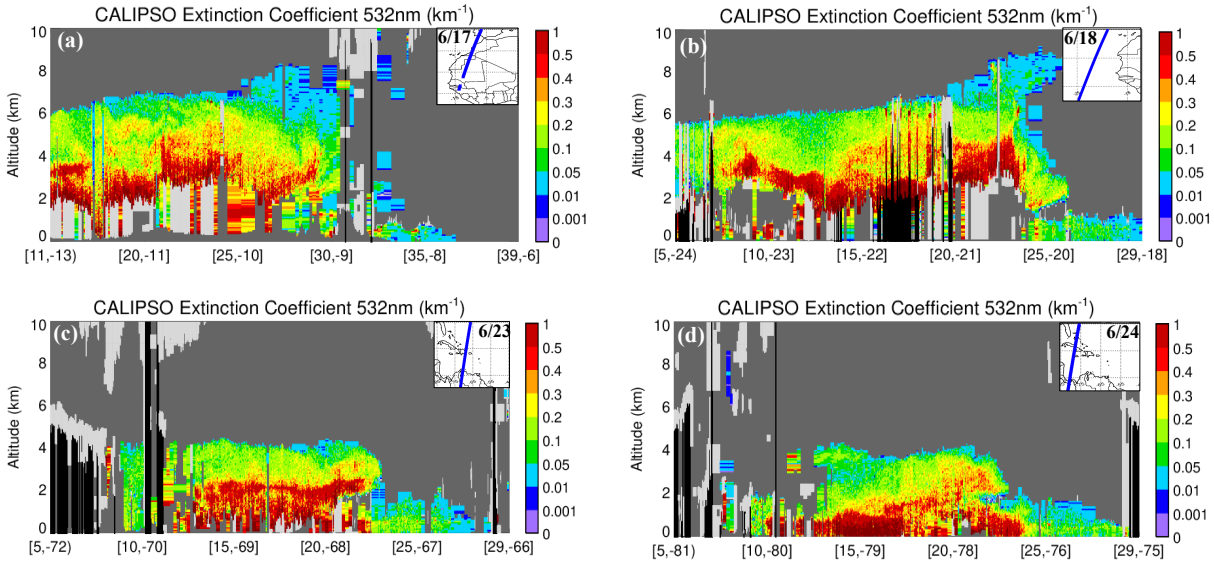

Figure 5: Curtains of CALIOP/CALIPSO aerosol extinction at 532 nm (colored) in North African coastal region (a – June 17, and b – June 18) and the Caribbean Basin (c – June 23, and d – June 24). Light gray, dark gray, and black represents cloudy, clear and clean (below the detection limit), and totally attenuated feature, respectively. X-axis denotes [latitude, longitude] of the CALIPSO track.

https://doi.org/10.5194/acp-2021-73
Preprint. Discussion started: 3 March 2021

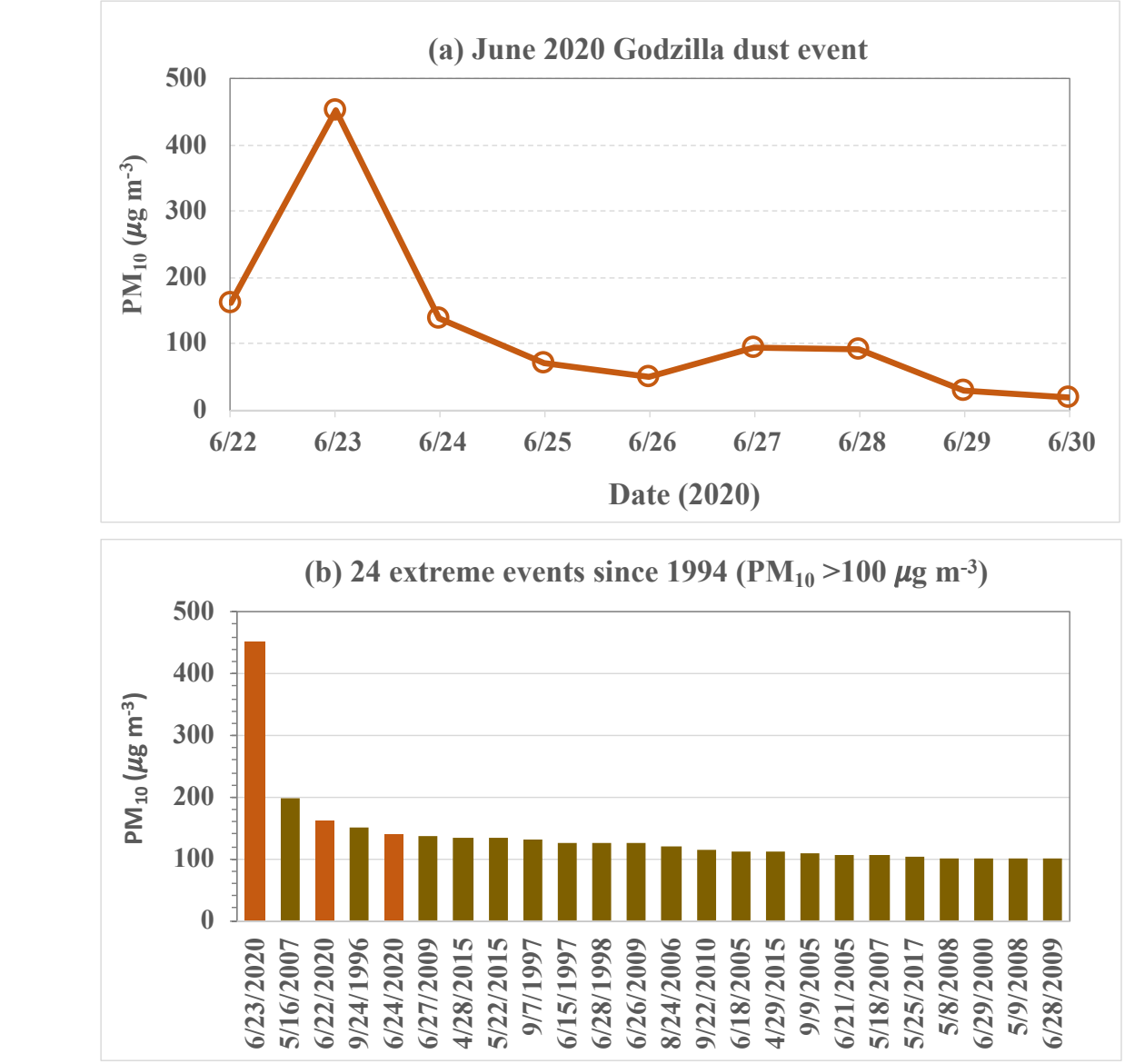

Figure 6: (a) PM_{10} concentration measured at Catano, Puerto Rico during the June 2020 dust event, (b) 24 extreme dust events (PM_{10} > 100 μg m^{-3}) at this site since 1994.

https://doi.org/10.5194/acp-2021-73
Preprint. Discussion started: 3 March 2021

Atmospheric Chemistry and Physics Discussions

700

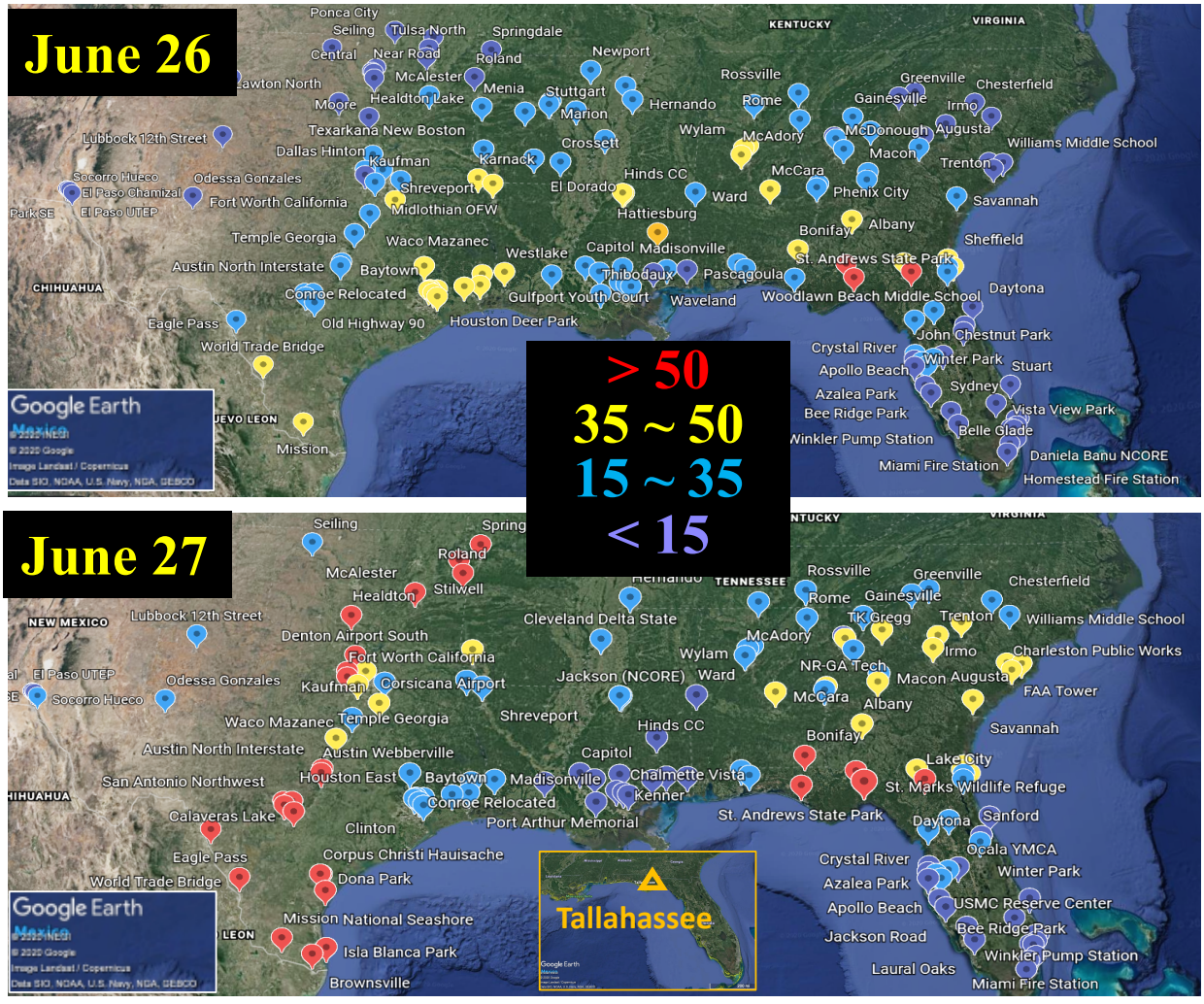

Figure 7: Observed $PM_{2.5}$ concentrations at the EPA air quality network over southern U.S. on June 26 (top) and 27 (bottom), respectively. $PM_{2.5}$ concentrations are categorized and marked with color into four ranges: <15 (purple), 15–35 (blue), 35–50 (yellow), and >50 (red) μg m^{-3}. Note that the EPA air quality standard for 24-hr $PM_{2.5}$ is 35 μg m^{-3}. Location of Tallahassee is shown in inset of the June 27 map. The background maps are copyrighted by © Google Earth.

https://doi.org/10.5194/acp-2021-73
Preprint. Discussion started: 3 March 2021

Atmospheric Chemistry and Physics Discussions

705

710

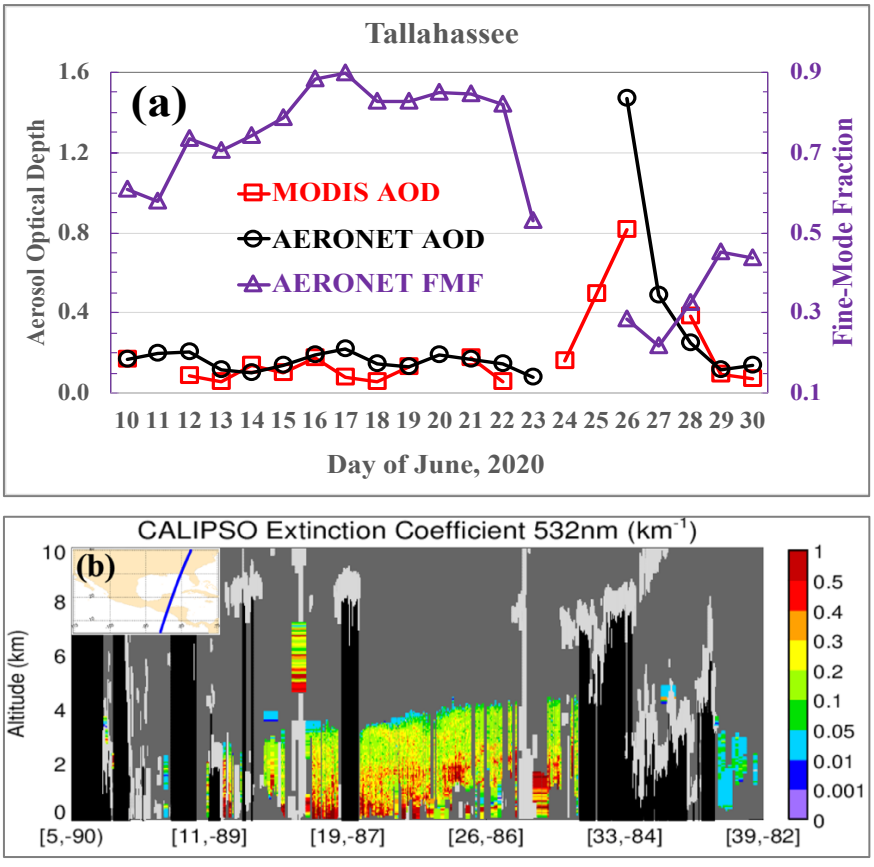

Figure 8: The intrusion of African dust into the Florida panhandle as evidenced in remote sensing observations: Left - evolution of AOD (black from AERONET and red from MODIS, left axis) and FMF (purple from AERONET, right axis) over Tallahassee, Florida during June 10-30, 2020; Right: curtain of CALIOP/CALIPSO aerosol extinction (at 532 nm) along a CALIPSO track overpassing the Florida panhandle on June 25, 2020. X-axis denotes [latitude, longitude] of the CALIPSO track.

https://doi.org/10.5194/acp-2021-73
Preprint. Discussion started: 3 March 2021

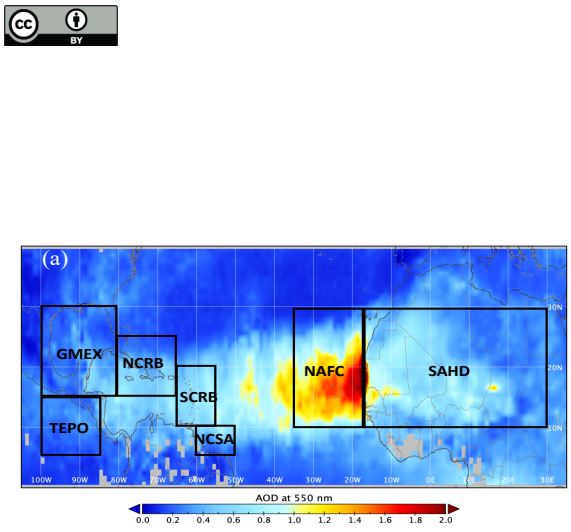

Atmospheric Chemistry and Physics Discussions

715

Figure 9: MODIS/Terra daily AOD for 2020 (red dot and thick line) in comparison to 2000-2019 climatology (the median and range of daily AOD are represented by thick black line and gray vertical bar, respectively) in seven regions defined in (a), including (b) NAFC, (c) SCRB, (d) NCRB, (e) NCSA, (f) GMEX, (g) TEPO, and (h) SAHD. The insets in (b-h) zoom in to the day-to-day variations of regional AOD from June 10 to June 30, 2020.

https://doi.org/10.5194/acp-2021-73
Preprint. Discussion started: 3 March 2021

Atmospheric Chemistry and Physics Discussions

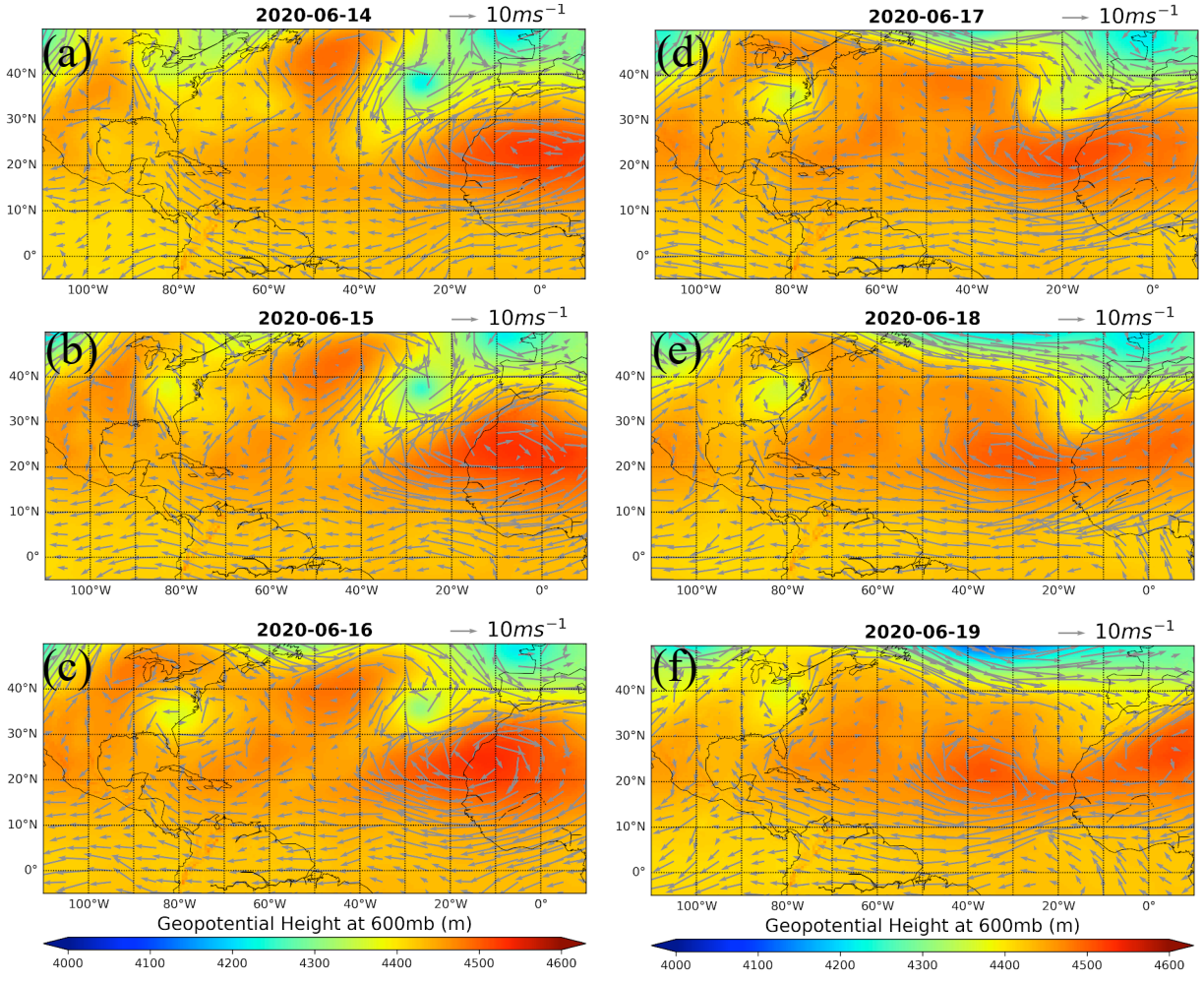

Figure 10: Patterns of MERRA2 geopotential height (color) and wind vector (gray arrow) at 600 hPa level on June 14(a), 15 (b), 16 (c), 17 (d), 18 (e), and 19 (f), 2020.

https://doi.org/10.5194/acp-2021-73
Preprint. Discussion started: 3 March 2021

Atmospheric Chemistry and Physics Discussions

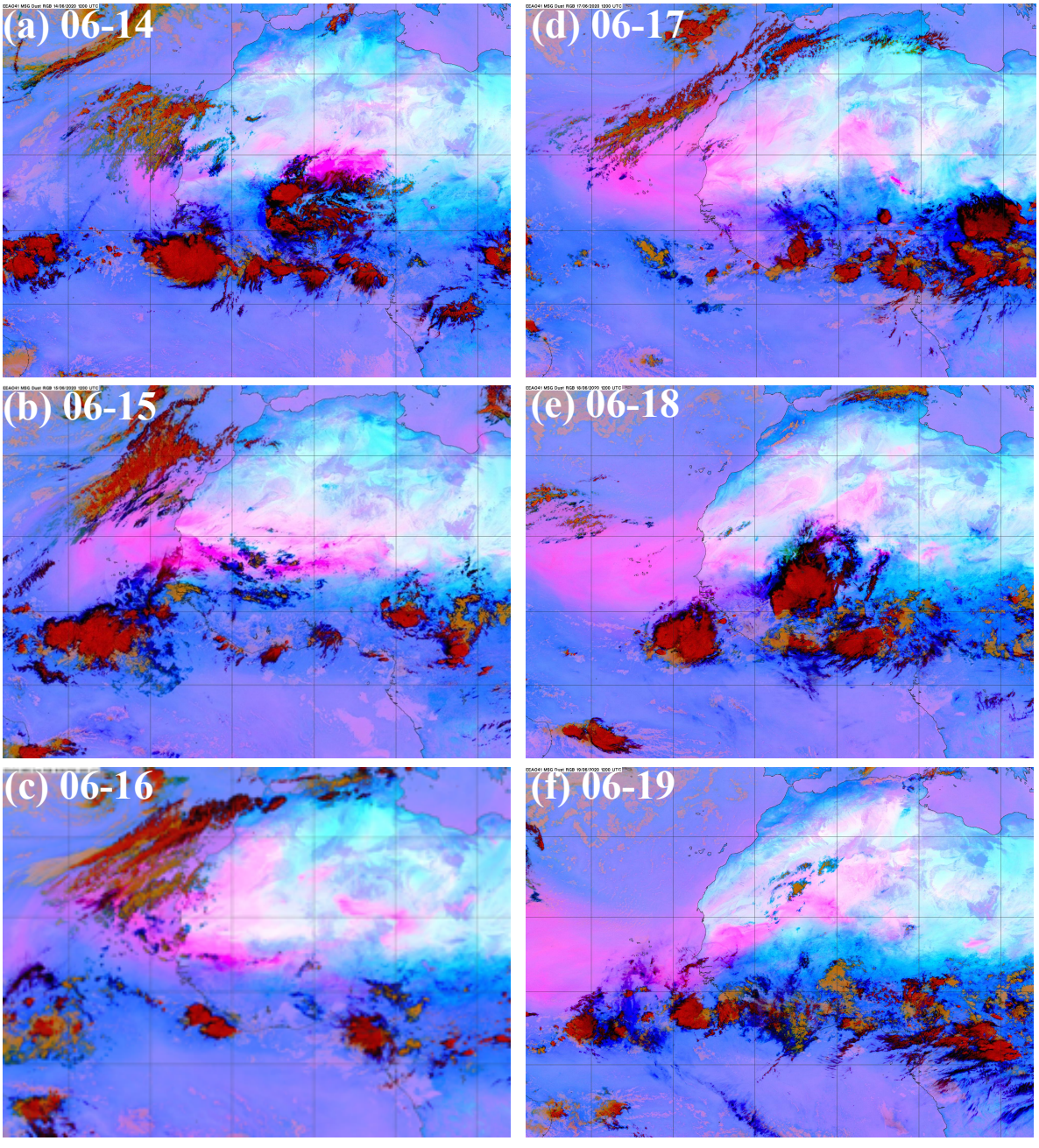

Figure 11: Coastal accumulation and ventilation of dust plumes (magenta) from haboobs (associated with mesoscale convection systems, dark red) and other meteorological processes in West Africa as revealed by SEVIRI RGB dust images at 12Z of (a) 06-14, (b) 06-15, (c) 06-16, (d) 06-17, (e) 06-18, and (f) 06-19. An animation of the SEVIRI images every 30 min covering June 12-25 can be played in SOM.

720

https://doi.org/10.5194/acp-2021-73
Preprint. Discussion started: 3 March 2021

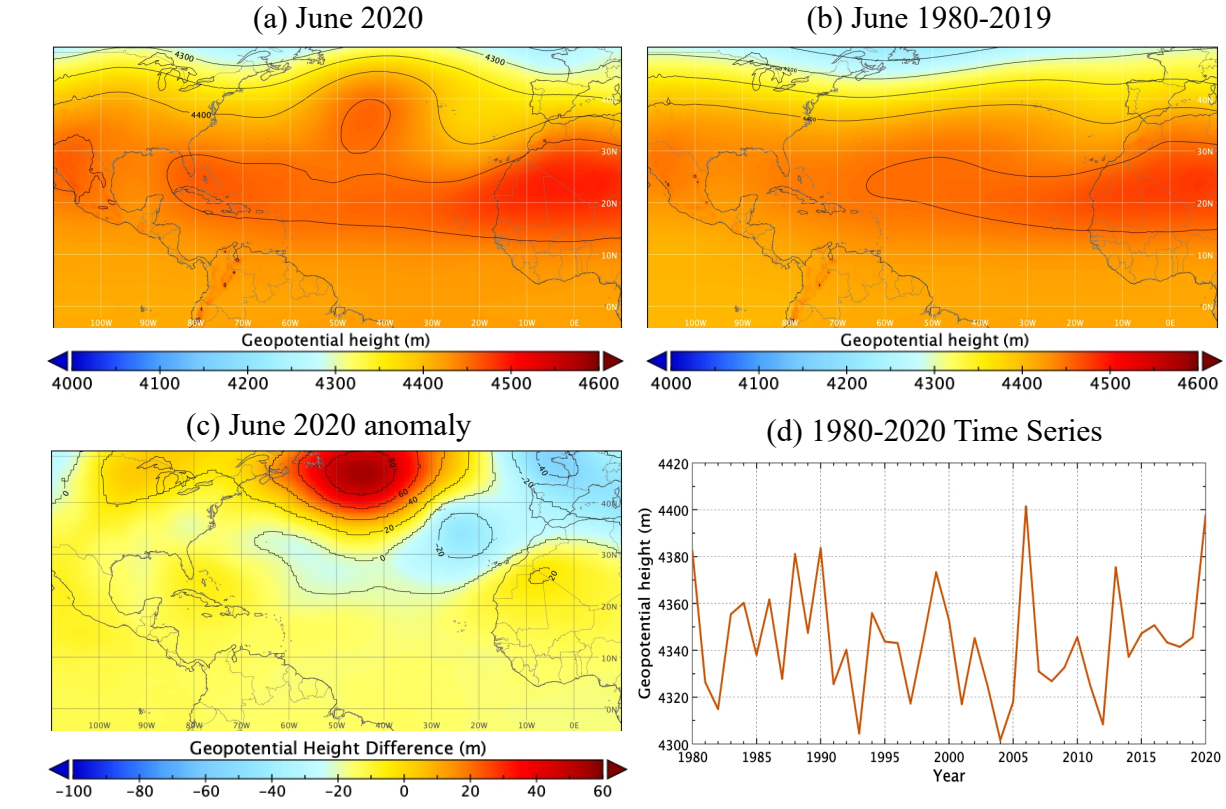

Figure 12: MERRA2 reanalysis geopotential height at 600 hPa: (a) June 2020, (b) June climatology (1980-2019), (c) June 2020 anomaly, and (d) 1980-2020 time series averaged over 35°N-50°N and 60°W-30°W.

725

https://doi.org/10.5194/acp-2021-73
Preprint. Discussion started: 3 March 2021

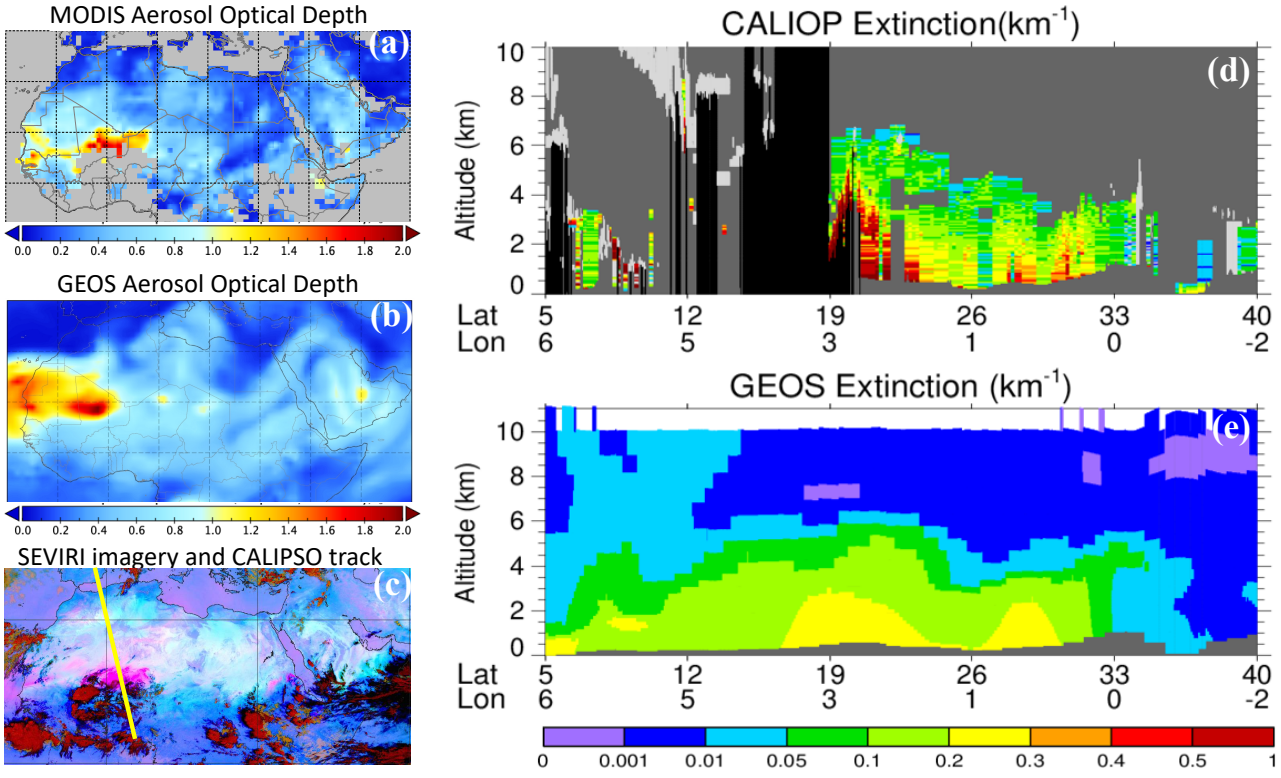

Figure 13: Satellite and GEOS characterizations of dust over North Africa on June 14, 2020: (a) MODIS AOD at 550 nm, (b) GEOS AOD at 550 nm, (c) SEVIRI RGB image with CALIPSO track (yellow line), altitude-latitude curtains of aerosol extinction coefficient (unit: km^{-1}) from CALIOP at 532 nm (d) and GEOS at 550 nm (e). Hourly GEOS outputs close to the satellite overpassing time are used.

https://doi.org/10.5194/acp-2021-73
Preprint. Discussion started: 3 March 2021

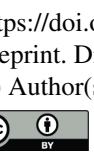

Atmospheric Chemistry and Physics Discussions

730

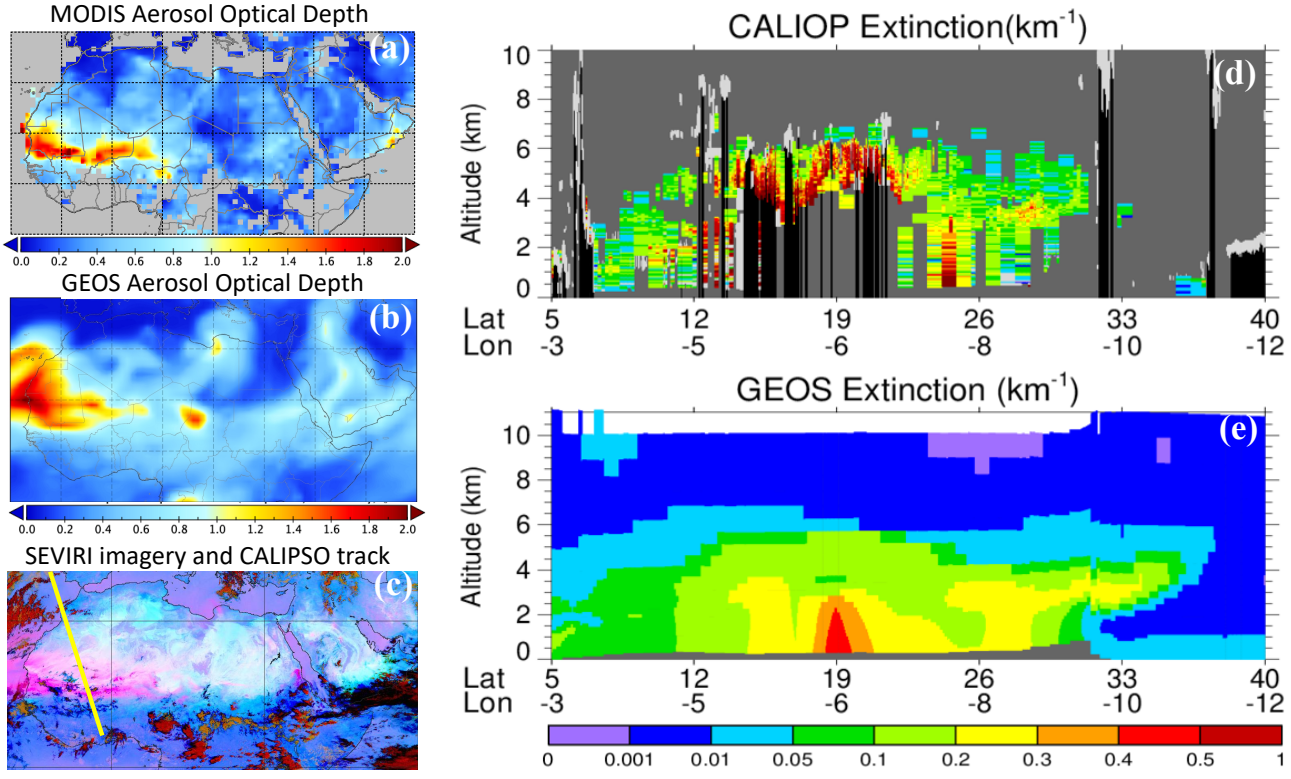

Figure 14: same as Figure 13 except for June 15, 2020.

https://doi.org/10.5194/acp-2021-73
Preprint. Discussion started: 3 March 2021

Atmospheric Chemistry and Physics Discussions

735

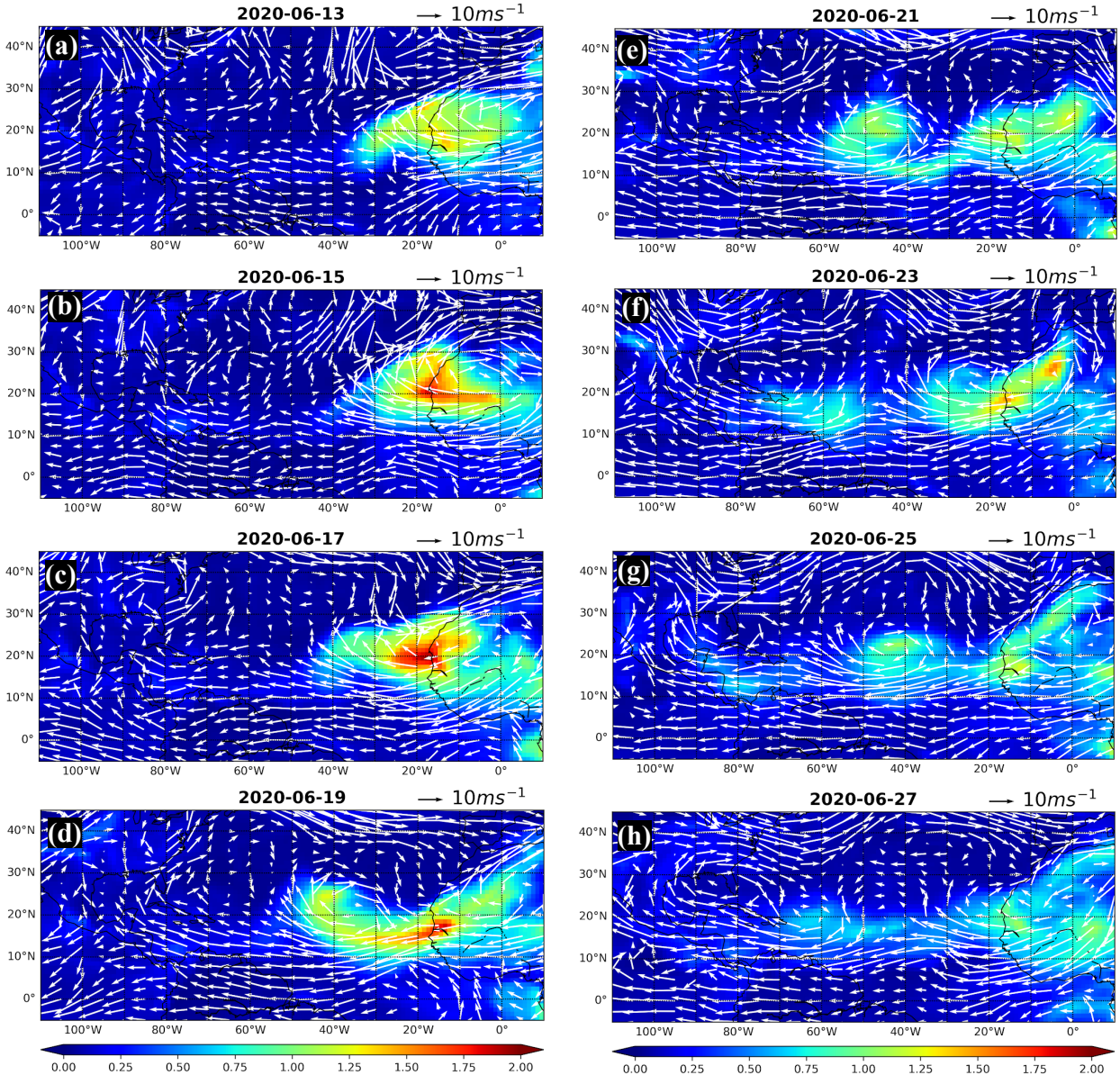

Figure 15: GEOS simulated evolution of trans-Atlantic AOD (color map) during the period of June 13-27, 2020. Overlaid on the AOD map is MERRA2 wind vectors at an altitude of about 4 km.

https://doi.org/10.5194/acp-2021-73
Preprint. Discussion started: 3 March 2021

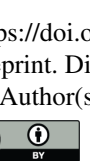

Atmospheric Chemistry and Physics Discussions

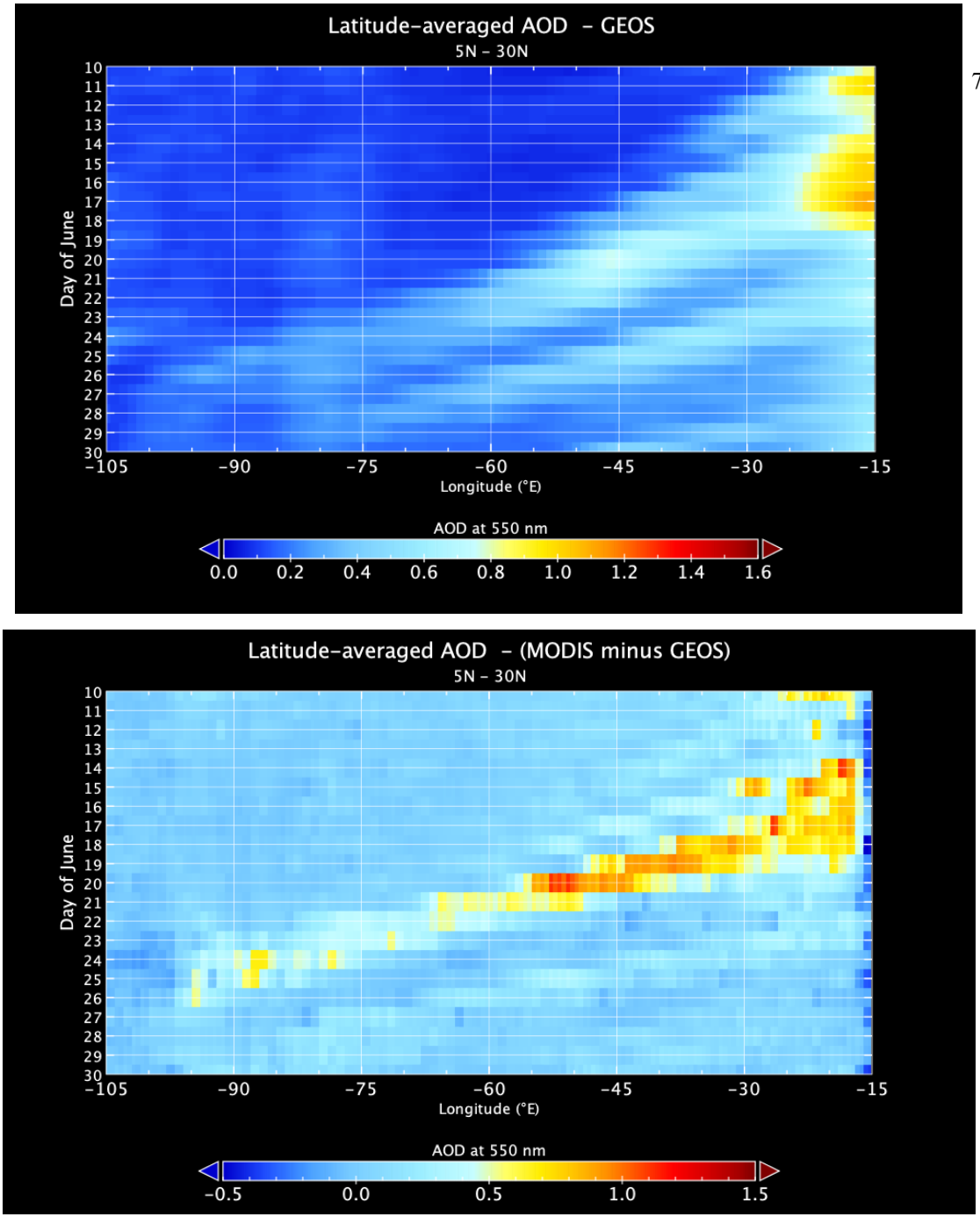

740

Figure 16: Time-longitude Hovmöller diagrams for GEOS latitude-averaged (5ºN-30ºN) AOD (top) and difference between MODIS and GEOS AOD (bottom).

https://doi.org/10.5194/acp-2021-73
Preprint. Discussion started: 3 March 2021

Atmospheric Chemistry and Physics Discussions

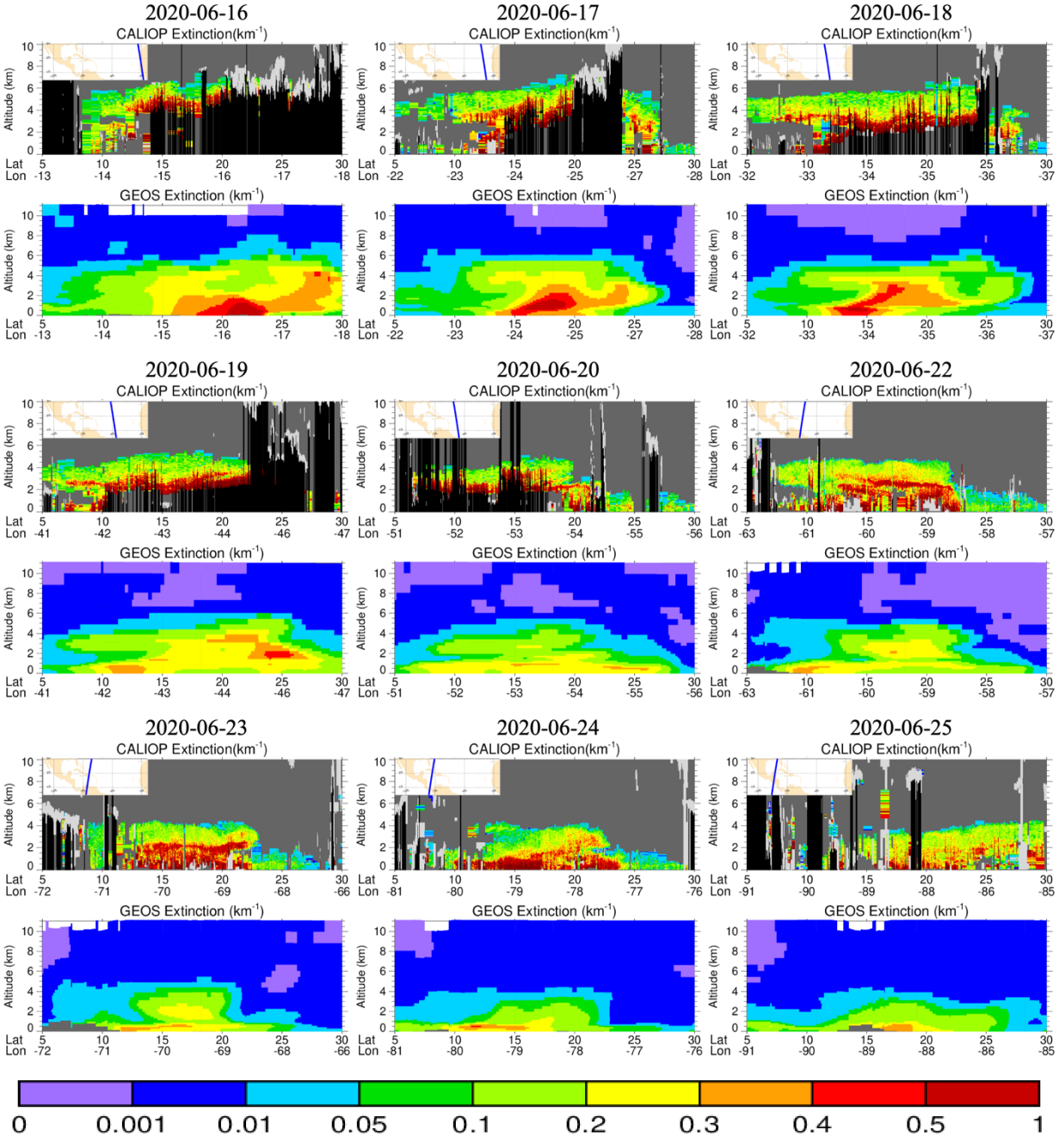

Figure 17: Comparison of altitude-latitude/longitude curtain of aerosol extinction coefficient (km^{-1}) between CALIOP (at 532 nm) and GEOS (at 550 nm) along the dust plume transit for 9 selected days. GEOS model outputs were sampled along the CALIPSO track shown as blue line overlying the geographical map (see insets). For CALIOP curtains, the cloudy scene, clear-clean scene, and totally attenuated feature is marked as light gray, dark gray, and black, respectively.

https://doi.org/10.5194/acp-2021-73
Preprint. Discussion started: 3 March 2021

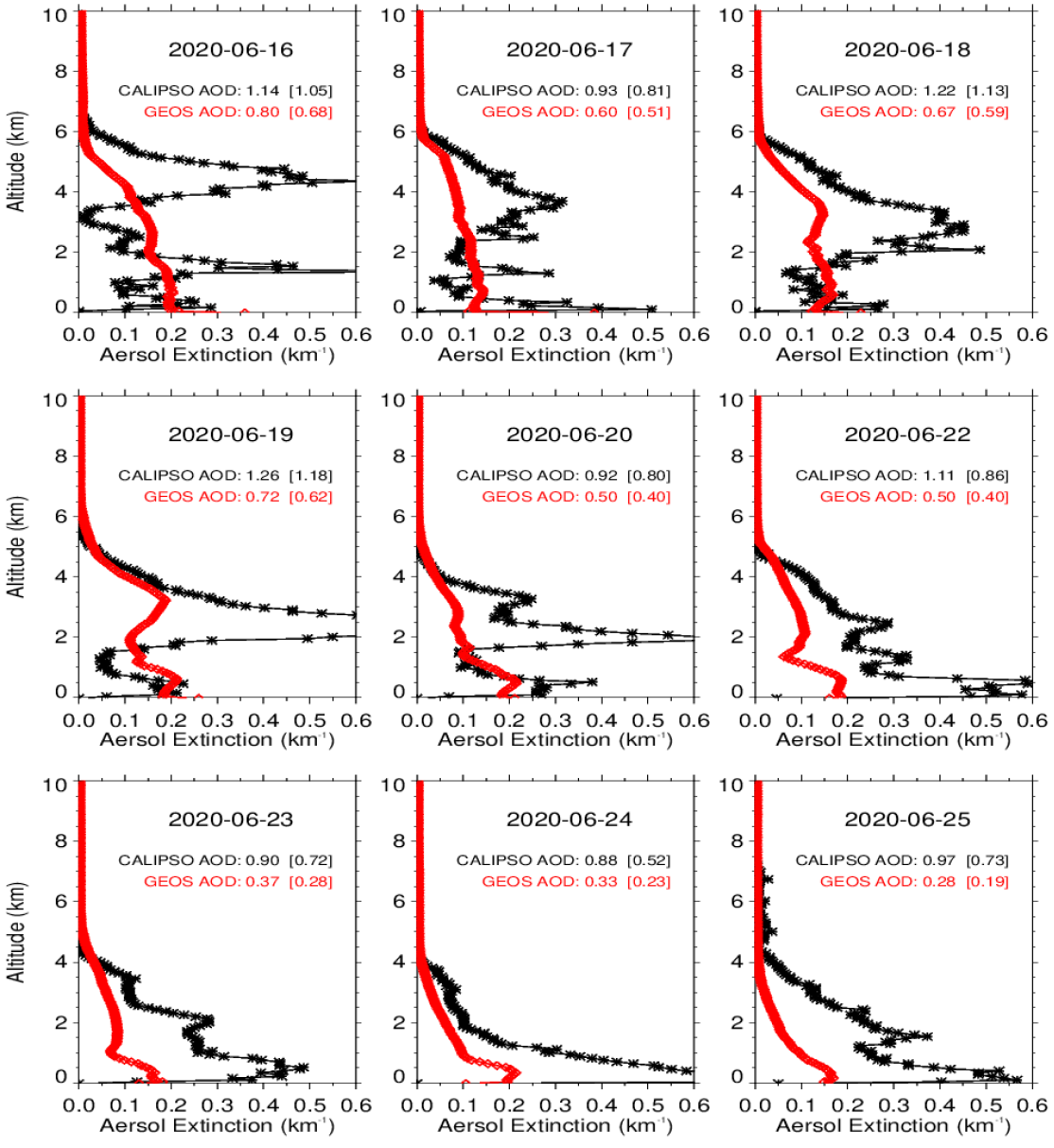

Figure 18: Latitude-averaged (5°N-30°N) aerosol extinction (km^{-1}) profiles from CALIOP (black) and GEOS (red) (corresponding to CALIPSO tracks illustrated in Figure 17), showing the evolution of vertical structure of the dust plume in the course of trans-Atlantic transport from the coast of North Africa (June 16) to the Gulf of Mexico (June 25). CALIOP AOD and GEOS AOD are also denoted in the plots (numbers in parentheses are AOD above the 500 m altitude). GEOS model outputs were excluded in the averaging when CALIOP detected clouds or the laser was totally attenuated (marked as light gray and black in Figure 17, respectively).